AMERICAN SOCIETY FOR MICROBIOLOGY | Journal of Bacteriology®

RESEARCH ARTICLE

A Novel Bvg-Repressed Promoter Causes *vrg*-Like Transcription of *fim3* but Does Not Result in the Production of Serotype 3 Fimbriae in Bvg⁻ Mode *Bordetella pertussis*

Qing Chen,[a] Gloria Lee,[a] Candice Craig,[a]* Victoria Ng,[a]* Paul E. Carlson, Jr.,[a] Deborah M. Hinton,[b] Scott Stibitz[a]

[a]Division of Bacterial, Parasitic, and Allergenic Products, Center for Biologics Evaluation and Research, FDA, Silver Spring, Maryland, USA

[b]Gene Expression and Regulation Section, Laboratory of Cell and Molecular Biology, NIDDK, National Institutes of Health, Bethesda, Maryland, USA

ABSTRACT In *Bordetella pertussis*, two serologically distinct fimbriae, FIM2 and FIM3, undergo on/off phase variation independently of each other via variation in the lengths of C stretches in the promoters for their major subunit genes, *fim2* and *fim3*. These two promoters are also part of the BvgAS virulence regulon and therefore, if in an on configuration, are activated by phosporylated BvgA (BvgA~P) under normal growth conditions (Bvg$^+$ mode) but not in the Bvg$^-$ mode, inducible by growth in medium containing $MgSO_4$ or other compounds, termed modulators. In the *B. pertussis* Tohama I strain (FIM2$^+$ FIM3$^-$), the *fim3* promoter is in the off state. However, a high level of transcription of the *fim3* gene is observed in the Bvg$^-$ mode. In this study, we provide an explanation for this anomalous behavior by defining a Bvg-repressed promoter (BRP), located approximately 400 bp upstream of the P*fim3* transcriptional start. Although transcription of the *fim3* gene in the Bvg$^-$ mode resulted in Fim3 translation, as measured by LacZ translational fusions, no accumulation of Fim3 protein was detectable. We propose that Fim3 protein resulting from translation of mRNA driven by BRP in the Bvg$^-$ mode is unstable due to a lack of the fimbrial assembly apparatus encoded by the *fimBC* genes, located within the *fha* operon, and therefore is not expressed in the Bvg$^-$ mode.

IMPORTANCE In *Bordetella pertussis*, the promoter P*fim3*-15C for the major fimbrial subunit gene *fim3* is activated by the two-component system BvgAS in the Bvg$^+$ mode but not in the Bvg$^-$ mode. However, many transcriptional profiling studies have shown that *fim3* is transcribed in the Bvg$^-$ mode even when P*fim3* is in a non-permissive state (P*fim3*-13C), suggesting the presence of a reciprocally regulated element upstream of P*fim3*. Here, we provide evidence that BRP is the cause of this anomalous behavior of *fim3*. Although BRP effects *vrg*-like transcription of *fim3* in the Bvg$^-$ mode, it does not lead to stable production of FIM3 fimbriae, because expression of the chaperone and usher proteins FimB and FimC occurs only in the Bvg$^+$ mode.

KEYWORDS *Bordetella pertussis*, Bvg-repressed gene, *fim3*, *vrg*

Whooping cough is a highly contagious human-restricted respiratory disease that is undergoing a resurgence. Despite extensive vaccination programs and good vaccine acceptance rates, over 48,000 cases of pertussis were reported in the United States in 2012 (1). Like many other Gram-negative pathogens, *Bordetella pertussis* produces a number of different macromolecules that mediate adherence to host cells, including filamentous hemagglutinin (FHA), fimbriae (FIM2 and FIM3), and pertactin. These factors have been demonstrated to play a role in animal models and cell culture and are believed to be involved in colonization and disease initiation in the mammalian

Received 23 March 2018 **Accepted** 27 July 2018

Accepted manuscript posted online 30 July 2018

Citation Chen Q, Lee G, Craig C, Ng V, Carlson PE, Jr, Hinton DM, Stibitz S. 2018. A novel Bvg-repressed promoter causes *vrg*-like transcription of *fim3* but does not result in the production of serotype 3 fimbriae in Bvg$^-$ mode *Bordetella pertussis*. J Bacteriol 200:e00175-18. https://doi.org/10.1128/JB.00175-18.

Editor Victor J. DiRita, Michigan State University

Address correspondence to Qing Chen, qing.chen@fda.hhs.gov.

* Present address: Candice Craig, Department of Biochemistry and Molecular Biology, Rutgers University, Piscataway, New Jersey, USA; Victoria Ng, Department of Cancer Biology, Vanderbilt University Medical Center, Nashville, Tennessee, USA.

host (2–5). Together with pertussis toxin, they are components of some current acellular pertussis vaccines (6).

In *B. pertussis*, fimbriae of two distinct serotypes, FIM2 and FIM3, are composed primarily of the major subunits Fim2 and Fim3, respectively, whose genes *fim2* and *fim3* are at unlinked chromosomal locations (7, 8). A silent *fim* locus is also encoded by *fimX*. However, the fimbrial accessory genes *fimBCD*, coding for the chaperone FimB, usher FimC, and minor subunit tip adhesin FimD, respectively, are located within, and cotranscribed with, the *fha* operon, driven by the promoter P*fha* (9, 10). The *fim* loci can independently undergo phase variation via alteration in the lengths of monotonic stretches of cytosine residues (C stretch) in their promoters, P*fim2*, P*fim3* (Fig. 1), and P*fimX*, presumably through slipped-strand mispairing during replication (11, 12). We have previously determined the length of the C stretch that allows maximal transcription for each promoter *in vivo*, represented by P*fim2*-12C, P*fim3*-15C, and P*fimX*-17C (13). The native conformations of these promoters in the Tohama I strain of *B. pertussis* (FIM2$^+$ FIM3$^-$) are P*fim2*-12C, P*fim3*-13C, and P*fimX*-7C (8, 13). The *fimX* locus is stably silent, presumably due to the inability of P*fimX* to expand from the wild-type C stretch length of 7 to a permissive length of 17.

Like other promoters of virulence genes, such as P*fha*, P*prn*, P*cya*, and P*ptx*, and of regulatory genes, such as P*bvgR* and P*bvgAS*, the C-stretch-optimized versions of the *fim* promoters (P*fim2*-12C, P*fim3*-15C, and P*fimX*-17C) were further shown to be transcriptionally activated by the global two-component response regulator BvgA (11, 13). BvgA is phosphorylated by the membrane-spanning sensor kinase BvgS under standard laboratory growth conditions, i.e., in the Bvg$^+$ mode (14, 15). Under these conditions, expression of a separate group of genes, known as the *vrg*s (16), is silenced in a manner that is dependent on BvgR (17). Transcription of *bvgR* is activated directly by BvgA~P binding to the promoter P*bvgR* (18). Somewhat atypically compared to other two-component sensor kinases, BvgS appears to be turned on, i.e., actively phosphorylating BvgA, in the absence of specific signals, with recent elegant biochemical, structural, and genetic studies supporting this view (19–25). However, BvgS can be turned off by addition of compounds such as $MgSO_4$ or nicotinic acid to the growth medium or by culture at lower temperatures (25°C), resulting in the Bvg$^-$ mode, a phenomenon known as modulation (26). Thus, in the Bvg$^-$ mode, the Bvg-activated genes are not expressed. However, due in part to the absence of BvgR expression, the *vrg*s are transcribed (18, 27).

The precise mechanism by which BvgR negatively regulates *vrg*s is not clear. Transcriptional activation of the *vrg*s requires RisA, another two-component response regulator in *B. pertussis* (27–29). In *B. pertussis*, mechanisms of regulation by RisA are not straightforward, since the neighboring gene for its presumptive cognate sensor kinase, RisS, is inactivated by frameshift mutation. The truncated RisS does not contribute to *vrg* regulation (28). Our recent work indicates that RisA is phosphorylated by cross talk with a noncooperonic histidine kinase, RisK (29).

In contrast to accumulated evidence that expression of extracellular fimbriae is a Bvg$^+$ mode trait (11, 13), the *fim3* gene, but not *fim2* or *fimX*, has been shown to be highly transcribed in the Bvg$^-$ mode in transcriptomic studies (30–32). All of these studies have been performed in the Tohama I genetic background, in which P*fim3* is in a nonpermissive configuration. Thus, in this context the *fim3* gene has been identified as a *vrg*, i.e., more highly expressed in the Bvg$^-$ mode than in the Bvg$^+$ mode.

In this study, we have identified a novel, highly active, highly regulated, *vrg*-like Bvg-repressed promoter (BRP), located approximately 400 bp upstream of the P*fim3* transcriptional start, as the cause of the observed *vrg*-like behavior of *fim3*. The ancestral function of the BRP is unclear. An open reading frame (ORF) is present downstream of it. However, that ORF, which we have designated *vrgX*, was apparently created relatively recently in evolution and is not present in strains of *B. bronchiseptica*. It is generally well accepted, based on molecular cladistics, that *B. pertussis* evolved from a common ancestor that was more *B. bronchiseptica*-like (33). In the context of such a timeline, *vrgX* was created in the lineage leading to *B. pertussis* by a 62-bp

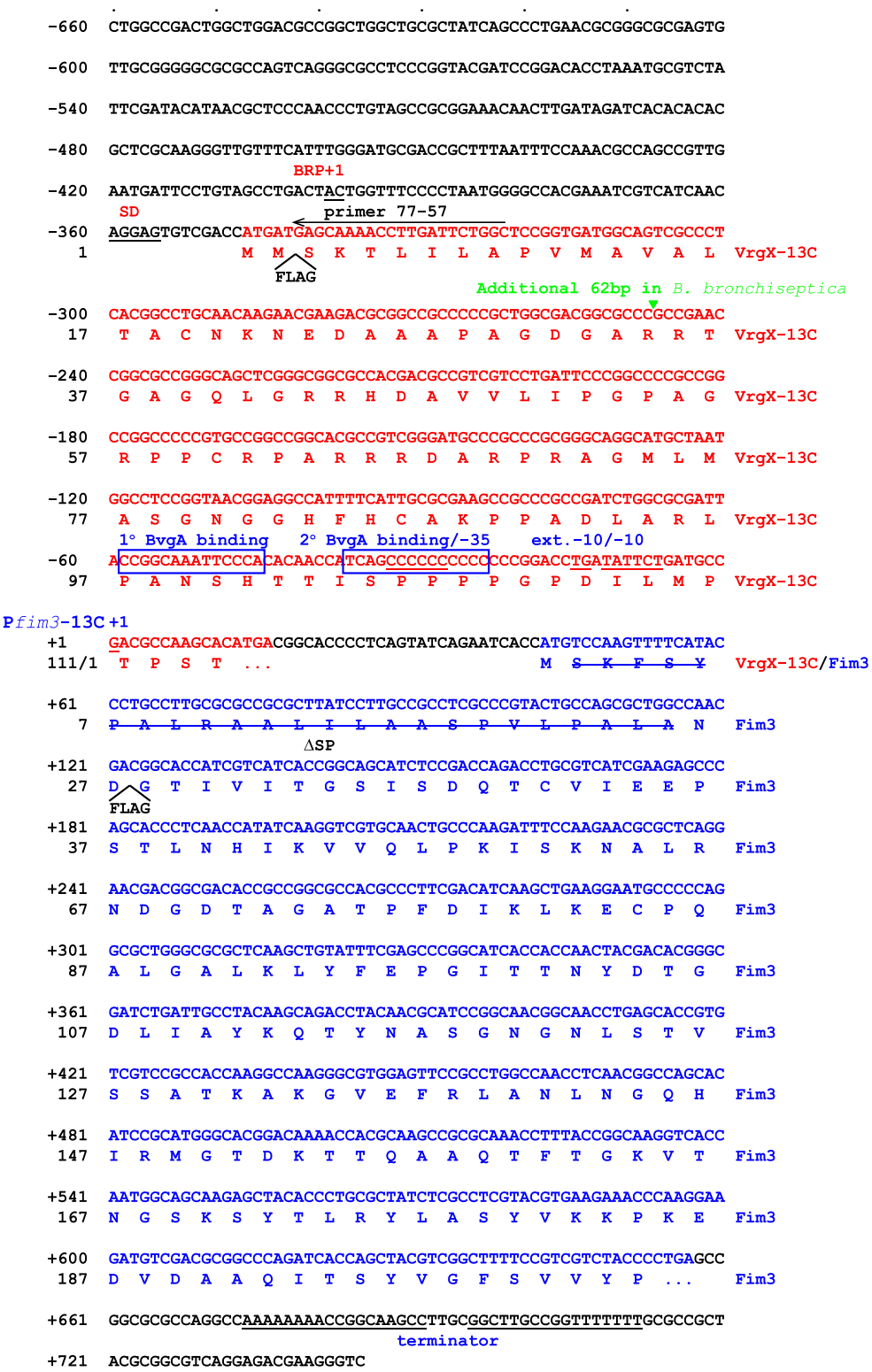

FIG 1 Sequence of the BRP-*fim3* region. Nucleotide sequence of the BRP-*fim3* region from *B. pertussis* Tohama I strain (P*fim3*-13C) (8), GenBank accession no. NC_002929.2, is numbered relative to the P*fim3* transcriptional initiation site at +1 (G), which was identified previously (13). The promoter elements, ORFs, and predicted amino acid sequences for VrgX-13C and Fim3 are in red and blue, respectively. The experimentally determined BRP transcription initiation sites (AC) and the putative Shine-Dalgarno (SD; AGGAG) sequence were identified in this study. The P*fim3* promoter elements (−10/extended −10) and the P*fim3* −35 region are underlined, as are the inverted repeat sequences making up the P*fim3* transcription terminator. The P*fim3* BvgA binding regions (primary and secondary) (13) are boxed. Strikeout of Fim3 amino acids indicates the deletion of the signal peptide (SP) from the constructs of pQC2182 (P*fim3*-13C-Fim3$_{\Delta SP}$) and pQC2188 (P*fim3*-15C-Fim3$_{\Delta SP}$). The positions of the FLAG tags for VrgX and Fim3 are indicated by labeled carets. An arrow above

(Continued on next page)

deletion that removed part of a highly GC-rich region (Fig. 1). However, the BRP apparently evolved in the absence of *vrgX*, as BRP structure and function is conserved in *B. bronchiseptica* strains in which *vrgX* is absent. We demonstrate here by translational fusion that transcription from BRP results in translation of *vrgX* but not in the accumulation of a stable protein product. Similarly, BRP drives transcription of the *fim3* gene and we detected the translation of *fim3* by gene fusion, but we did not detect production of serotype 3 fimbriae in the Bvg$^-$ mode. In the latter example, this may be due, at least in part, to the lack of expression of the accessory *fimBCD* genes, which are embedded in the operon for filamentous hemagglutinin and expressed only in the Bvg$^+$ mode. We speculate that transcription and resulting translation from BRP is a novel aspect of *B. pertussis* biology that represents an evolutionary fossil stemming from its divergence from the *B. bronchiseptica*-like ancestor or may provide an as-yet unidentified function in the Bvg$^-$ mode.

RESULTS

***vrg*-like P*fim3* transcription in *B. pertussis*.** Previously, we created an ectopic promoter assay vector, pSS3967, containing a 1.8-kb *B. pertussis* chromosomal fragment that mediates insertion of this vector, by homologous recombination, in single copy into the *B. pertussis* genome at a specific location (13), as illustrated in Fig. S1A in the supplemental material. We previously used this vector to examine transcription from short promoter fragments containing P*fim3* and P*fim2* (−130 to +33 and −130 to +32 relative to the +1 position, respectively) as revealed by expression of the *luxCDABE* operon, leading to bioluminescence as a measurable output. In this way, we demonstrated that the C-stretch-optimized promoters, P*fim3*-15C and P*fim2*-12C, are Bvg activated *in vivo*. In contrast, nonpermissive promoters, such as P*fim3*-13C and P*fim2*-10C, displayed no detectable transcriptional activity. This approach has allowed us to compare different promoters, e.g., P*fim*2, P*fim3*, P*fimX*, P*fha*, and P*ptx*, in an identical, albeit isolated, genetic context regardless of their native locations or contexts in the *B. pertussis* chromosome. In this assay P*fim3* behaved as a typical Bvg-activated gene (*vag*) (13, 15).

However, transcriptional profiling of the *B. pertussis* Tohama I strain and its derivative, BPSM, has revealed that *fim3* behaves as a Bvg-repressed gene (*vrg*) (30–32). This was particularly intriguing because the *B. pertussis* Tohama I strain is known to have a FIM2$^+$ FIM3$^-$ phenotype, in keeping with the reported status of the phase-variable *fim* promoters, i.e., P*fim2*-12C (on) and P*fim3*-13C (off) (11, 13). To begin to understand these anomalies in *fim3* gene transcription, we created a promoter assay vector, pSS4162, to measure transcriptional activity at defined points *in situ*. The plasmid vector pSS4162 (Fig. S1B) is devoid of the 1.8-kb *Bordetella* chromosomal fragment that directs insertion, at an ectopic location, by homologous recombination but is otherwise identical to pSS3967. For these experiments, the segments that direct insertion are cloned upstream of the *luxCDABE* operon and include sequences that are upstream of, and contiguous with, the promoter in its native context. After homologous recombination between the plasmid and chromosomal copies of these sequences, the rightmost end of the cloned fragment will define the fusion point at which transcription is being monitored, with all sequences upstream of that point being the same as that in the native genetic context. For creating such fusions, we typically use a 1-kb fragment in which the promoter of interest is at the right end. To measure the transcriptional activities of P*fim2* and P*fim3* in *B. pertussis*, fragments encompassing such sequences from *B. pertussis* Tohama I strain BP536 (FIM2$^+$ FIM3$^-$), namely, −988 to +32 for P*fim2*-12C and −945 to +33 for P*fim3*-13C, were used (Fig. S2). These *in situ lux* transcriptional fusions were designated P*fim2*-12C^{+32} and P*fim3*-13C^{+33}. In the *B.*

FIG 1 Legend (Continued)
the nucleotide sequence indicates the extent and direction of primer 77-57, used in primer extension. The position at which a specific 62-bp additional sequence (CGGCCACGACGGCCCCGGCTCCTTCGGCCCCCGCGCCCGCGCCTGCGCCGGCT CCCTCGCCC) present in *B. bronchiseptica* is indicated in green.

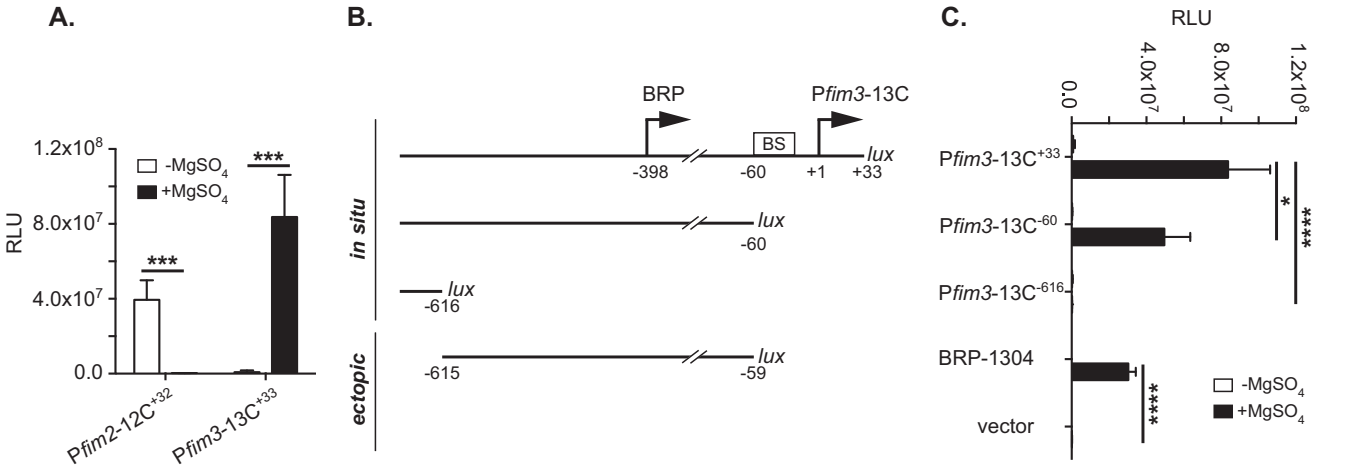

FIG 2 BRP results in *vrg*-like transcription of P*fim3* in *B. pertussis*. (A) Levels of luciferase activity directed by P*fim2* and P*fim3* cloned from BP536 (FIM2$^+$ FIM3$^-$) as 1-kb fragments into the *lux* transcriptional assay vector pSS4162 and integrated *in situ*. The DNA sequences of the *in situ lux* fusions for P*fim2*-12C^{+32} and P*fim3*-13C^{+33} are shown in Fig. S2. (B) Diagrammatic representation of fusion points with the *lux* operon in *B. pertussis* BP536 strains harboring pSS4162 with various BRP-*fim3* regions integrated into the chromosome (*fim3*-13C^{+33}, P*fim3*-13C^{-60}, and P*fim3*-13C^{-616}). The fusion points are represented by the rightmost sequence coordinate, numbered relative to the transcription start at +1 in P*fim3*-13C. The BvgA binding region (BS) is indicated. BRP-1304 harbors the P*fim3* upstream region (−615 to −59) cloned into the *lux* transcriptional assay vector pSS3967 and integrated at an ectopic location. (C) *B. pertussis* BP536 strains harboring chromosomally integrated derivatives of pSS4162 or pSS3967 were grown on BG agar in the absence or the presence of 50 mM $MgSO_4$ and analyzed for light production as described in Materials and Methods. The superscripted number indicates the promoter-*lux in situ* fusion point, corresponding to panel B, relative to the P*fim3*-13C transcriptional start. Values are given in arbitrary units (RLU, for relative luminescence units). Data averaged from at least four assays were used in the calculation of standard deviations, as indicated by error bars, and in the statistical analysis by unpaired two-tailed *t* test between two samples or by one-way ANOVA when P*fim3*-13C^{-60} and P*fim3*-13C^{-616} were compared to the control, *fim3*-13C^{+33}. *, $P \leq 0.05$; ***, $P \leq 0.001$; ****, $P \leq 0.0001$.

pertussis strain BP536 background, as expected and as shown in Fig. 2A, without $MgSO_4$ (Bvg$^+$ mode), the permissive promoter P*fim2*-12C^{+32} was active, whereas the nonpermissive promoter P*fim3*-13C^{+33} was inactive. When $MgSO_4$ was included in the growth medium to induce the Bvg$^-$ mode, activity from the permissive promoter P*fim2*-12C^{+32} was abolished. However, transcriptional activity downstream of the nonpermissive P*fim3*-13C^{+33} increased dramatically. We hypothesized that this high level of Bvg-repressed transcription was driven not by P*fim3* but by a Bvg-repressed promoter upstream of P*fim3*.

Mapping of the novel Bvg-repressed promoter BRP located upstream of P*fim3*. To determine if a Bvg-repressed promoter was present upstream of P*fim3*, we used the *in situ lux* fusion vector pSS4162 to fuse the *luxCDABE* operon at a point 60 bp upstream of the P*fim3*-13C transcriptional start (P*fim3*-13C^{-60} in Fig. 2B). Based on our previous study that mapped the BvgA-binding region of P*fim3* to between −60 and −25, this fusion lacks those upstream BvgA-binding sequences as well as core promoter elements of P*fim3* (13). As predicted by our hypothesis, this fusion was not transcribed in the Bvg$^+$ mode (−$MgSO_4$) (Fig. 2C) but, like P*fim3*-13C^{+33}, was highly transcribed in the Bvg$^-$ mode (with $MgSO_4$), indicating the presence of a Bvg-repressed promoter, which we named BRP, upstream of that point and therefore upstream of P*fim3*. A fusion of *lux* to a point further upstream (bp −616 relative to the P*fim3*-13C start, or P*fim3*-13C^{-616}) did not display this $MgSO_4$-induced transcription. The BRP thus appeared to reside within the region between positions −615 and −59 relative to P*fim3* +1. To confirm the presence of a Bvg-repressed promoter element, we cloned this region (−615 to −59) (Fig. 2B and Fig. S3, BRP-1304) into the ectopic *lux* transcription assay vector pSS3967, which was then integrated at the ectopic location. As shown in Fig. 2C, the BRP-1304 fragment displayed $MgSO_4$-dependent transcriptional activity relative to the negative control of the empty pSS3967 vector. These results support our hypothesis of the presence of a BRP that affects strong transcription downstream of *fim3* by read-through in the Bvg$^-$ mode.

To more accurately map the boundaries of BRP, we constructed deletions in the BRP-1304 fragment and assessed their effects on BRP activity in the ectopic location. As

shown in Fig. S4A, deletions up to bp −158 (BRP-1342), −258 (BRP-1341), or −358 (BRP-1340) from the right side of the fragment in BRP-1304 did not significantly impact transcriptional activity, but a similar deletion to bp −458 (BRP-1339) decreased expression to 6.6% of that of the starting fragment. Deletions from the left side up to bp −460 (BRP-1331) severely reduced activity, while a left-side deletion to bp −560 (BRP-1332) did not. These deletions indicated that the 203 bp from −560 to −358 contained essential BRP elements. A fragment encompassing these 203 bp, as in BRP-1406, retained 50% of BRP-1304 activity and served as the starting fragment for a second round of deletions, shown in Fig. S4B. In this round of incremental deletions of 20 bp, each successive deletion, from either side, reduced activity somewhat, but only after deletion of 60 bp from the left (BRP-1409) or 40 bp (BRP-1413) from the right did activity drop to essentially zero. In this round, the endpoints of the largest deletions that did not completely abolish activity defined a fragment of 123 bp (−520 to −398 [BRP-1653]) that retained 11.9% of the activity of BRP-1304 (Fig. S4B). It should be noted that although the level of activity of BRP-1653 was reduced relative to that of BRP-1304, it, like all other deletion constructs with partial activity, retained full regulation, as its activity was eliminated when grown in medium lacking $MgSO_4$. It therefore appears that this fragment encompasses core elements responsible for regulated expression while larger fragments contain sequences that augment its activity.

Determining the transcriptional start of BRP by primer extension. We speculated that the BRP transcriptional start was near nucleotide (nt) −398, because deletions from the right that extended into the core BRP farther than that essentially eliminated activity. To precisely locate the BRP transcriptional start, we performed primer extension analysis with total RNA prepared from different *B. pertussis* strains. Using primer 77-57 complementary to nucleotides −322 to −342 upstream of P*fim3* and priming toward BRP, as illustrated in Fig. 1 and 3A, RNA isolated from wild-type *B. pertussis* strain BP536 (P*fim3*-13C) generated a 77-nt product only in the presence of $MgSO_4$ (Fig. 3B, lane 4). To further validate this finding, we created a BP536 derivative strain, QC3980, in which P*fim3*-13C was changed to P*fim3*-15C through allelic exchange. QC3980 (P*fim3*-15C) produced the same primer extension product as that of BP536, only in the presence of $MgSO_4$ (Fig. 3B, lane 6), thus confirming that this product was independent of the activity of P*fim3*. The *in vitro* transcription products from a plasmid-encoded promoter, P*tac*, were included as a reference in each reaction (Fig. 3B). To more precisely localize the transcriptional start of BRP, we used a *B. pertussis* strain containing the ectopic *lux* fusion BRP-1340 (Fig. 3A) in which the cloned promoter fragment contained nucleotides −615 to −358 and therefore a functional BRP (Fig. S4A). As a negative control, we included a *B. pertussis* strain containing the ectopic *lux* fusion BRP-1339 (Fig. 3A) in which the cloned promoter fragment contains nucleotides −615 to −485, which are insufficient to provide a functional BRP (Fig. S4A). Primers BRE-2 and 1340 are both complementary to sequences within the *lux* operon of pSS3967 and prime backwards toward the SalI site at the 3′ end of cloned promoter sequences (Fig. 3A). As expected, RNA from the *B. pertussis* strain carrying BRP-1339 did not generate a primer extension product when primer 1340 was used (Fig. 3B, lanes 1 and 2). However, when primed with BRE-2, the RNA from the *B. pertussis* strain carrying BRP-1340 generated two primer extension products, of approximately 63 nt, only when that strain was grown in the presence of $MgSO_4$ (Fig. 3C, lanes 1 and 2). To unambiguously determine the starting nucleotide of BRP, plasmid pQC1340, encoding the BRP-1340 *lux* fusion, was used to generate a DNA sequence ladder that was then run alone (Fig. 3C, lanes 3 to 9) or doped with primer extension products generated using RNA from the BRP-1340 *lux*-containing strain grown without or with $MgSO_4$ in the medium (Fig. 3C, lanes 10 and 11). The two primer extension products were thus shown to correspond to the two start sites A and C, i.e., nt −398 and −397. These positions correspond closely to the 3′-end boundary of BRP mapped by deletion to the vicinity of nt −398 (BRP-1412 and BRP-1653) (Fig. S2B). Taken together, these data indicate the presence of a previously unrecognized Bvg-repressed promoter, BRP, located upstream

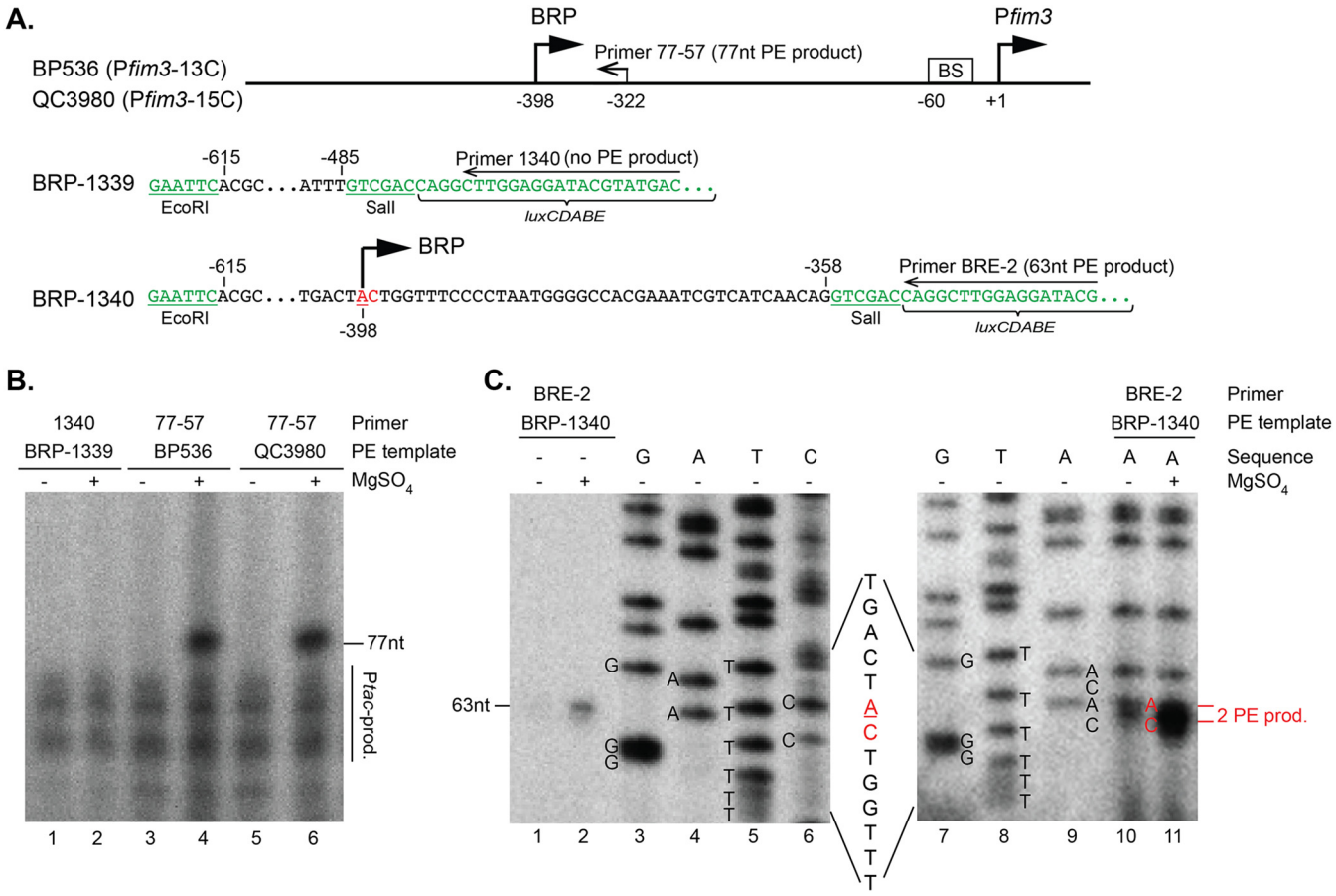

FIG 3 BRP primer extension and transcriptional start. (A) Diagrams and sequences of templates and primers used in primer extension (PE). Large arrows with solid heads indicate the starts and the directions for transcription from BRP and P*fim3*. Smaller arrows indicate locations and directions for primers, with the predicted sizes of PE products provided in parentheses. The location of the BvgA-binding region (BS) is indicated. The DNA sequences of the ends of the BRP-1339 (−615 to −485) and BRP-1340 (−615 to −358) fragments (black) are shown in context after cloning between the EcoRI and SalI sites of pSS3967 (green). Within BRP-1340, the BRP transcription start sites determined by these analyses are shown in red. (B and C) Gels showing PE products obtained using the indicated primers and RNA isolated from the indicated strains grown in the presence or absence of 50 mM $MgSO_4$. (B) P*tac* RNA prepared *in vitro* and a ^{32}P-labeled P*tac* primer that anneals 66 nt from the start of the P*tac* RNA were added to the primer extension analyses of BRP RNA as a control. (C) Sequencing ladder lanes (G, A, T, or C), which were generated by using 5′-^{32}P-labeled primer BRE-2 (lanes 3 to 6) or BRP-1340 (lanes 7 to 11), are depicted alone or mixed with primer extension product (lanes 10 and 11) to show precise location of the initiation nucleotide. The sequence within this region is indicated. Two BRP transcription starts (AC) are in red, with the major start site (A) underlined.

of P*fim3* and directing transcription initiating at nucleotides −397 and −398. Although this is the minimal element that demonstrated the regulatory phenotype of interest, to ensure the inclusion of all possible stimulatory elements, we used BRP-1304 as a full-length BRP in our subsequent efforts to understand the mechanisms of BRP regulation.

BRP is regulated similarly to other *vrgs*. Because BRP was induced under modulating conditions, we speculated that BRP belongs to the *vrg* family, i.e., that it is regulated in a fashion mechanistically similar to that demonstrated for classical *vrg*s such as *vrg-6*, *vrg-18*, *vrg-24*, and *vrg-73*. To investigate this possibility, we introduced an ectopic BRP-1340–*lux* fusion in *B. pertussis* strains harboring deletions of genes previously shown to affect *vrg* regulation. As a comparator and positive control, we introduced a similar *lux* fusion into P*vrg-73*, a strong *vrg* promoter. As shown in Fig. 4A and B, a deletion of *bvgR* led to derepression of both BRP-1304 and P*vrg-73*, even in the Bvg^+ mode, conditions under which their expression is eliminated in the wild-type strain. Derepression was to a level approximately half of the level observed in the wild-type strain under *vrg*-inducing conditions, i.e., when $MgSO_4$ is added to the medium. A similar pattern was observed with a Δ*bvgA* deletion strain, consistent with

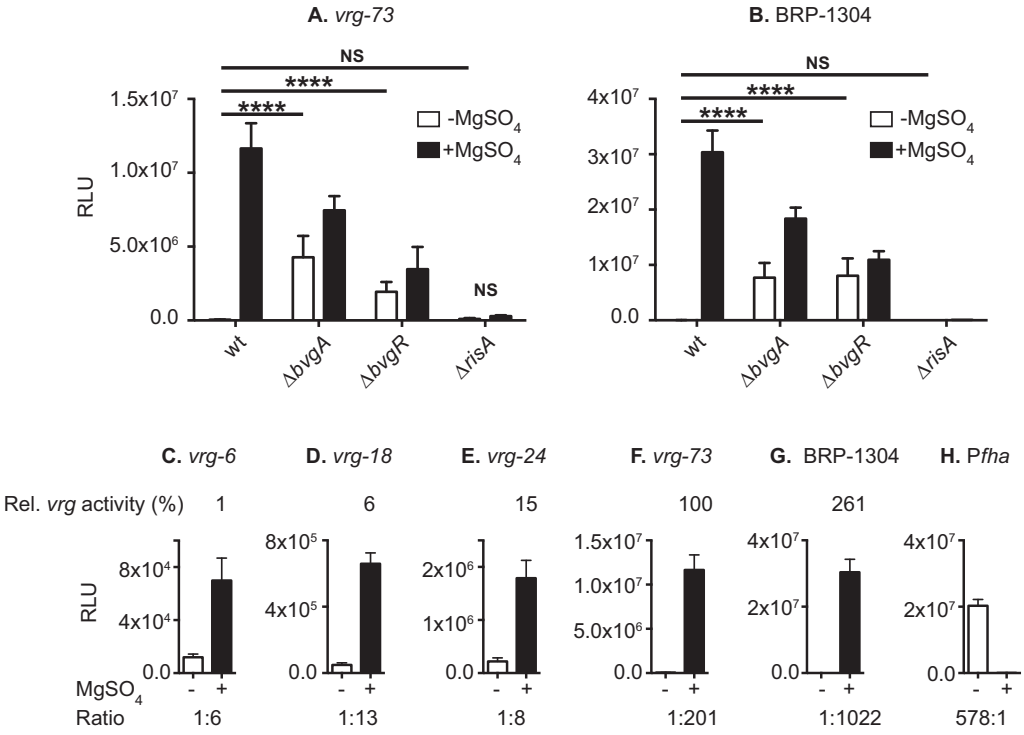

FIG 4 BRP is a strong and highly regulated *vrg*-like promoter in *B. pertussis*. The activities of ectopic *lux* transcriptional fusions to BRP-1304 or other *vrg* or *vag* promoters were assessed in wild-type and mutant strains, grown in the absence or presence of 50 mM $MgSO_4$ and analyzed for light production as described for Fig. 2. (A and B) Luciferase activity driven by the *vrg-73* promoter or BRP-1304 was assessed in four different genetic backgrounds (wild-type [wt] and Δ*bvgA*, Δ*bvgR*, and Δ*risA* mutants). Data averaged from 4 replicates were subjected to statistical analysis by unpaired two-tailed *t* test between two samples. NS (not significant), $P > 0.05$; *, $P \leq 0.05$; ***, $P \leq 0.001$; ****, $P \leq 0.0001$. (C to H) Different *vrg* promoters and the *vag* promoter P*fha* were assessed in the wild-type background. Comparison of *vrg* activity is relative (Rel.) to that of *vrg-73*, set at 100%. Ratios given below the graphs for individual promoters are the ratios between growth in the absence (−) or presence (+) of 50 mM $MgSO_4$.

the fact that *bvgR* is a BvgAS-activated gene. Although the overall level of derepressed expression did not equal that of the Bvg^- mode wild type, it should be kept in mind that in each of these mutants, a large number of genes, specific to the Bvg^- mode, is expressed. The diverse nature of these genes, recently catalogued by whole-genome transcriptome sequencing (RNA-seq), indicates that major physiological differences are experienced relative to the wild-type Bvg^+ mode (32). Therefore, it is not surprising that wild-type and mutant expression levels are not exactly the same. It should also be noted that this overall pattern and the relative levels for *vrg-73*, shown here to be similar to those for BRP-1304, are very similar to those reported previously for a Δ*bvgR* strain (27). In addition to this derepression observed in Δ*bvgA* or Δ*bvgR* mutant strains, mechanistic similarity of the regulation of BRP-1304 and *vrg-73* was also demonstrated by the dependence of each on the integrity of the *risA* gene. RisA has previously been shown to be required as a transcriptional activator of the *vrg*s (27–29).

Different *vrg*s display different levels of expression, as well as different degrees of responsiveness, i.e., different induction ratios, in response to modulation (16, 30–32). For example, transcriptome analyses (30, 32) have indicated that *vrg-73* is induced to a higher level than *vrg-6* by the addition of $MgSO_4$. We compared BRP-1304 to other known *vrg* promoters, i.e., those of *vrg-6*, *vrg-18*, *vrg-24*, and *vrg-73*, by *lux* transcriptional fusions in an ectopic genetic context, using pSS3967 as described above. As expected, transcription from the promoters of all the *vrg*s and BRP-1304 was highly induced in the presence of $MgSO_4$ (Fig. 4C to G), whereas transcription from the *vag* promoter P*fha* was regulated in an inverse fashion to these, being reduced 578-fold in the presence of $MgSO_4$ (Fig. 4H). This reflects the presence of significant amounts of phosporylated BvgA (BvgA~P) under standard growth conditions and elimination of

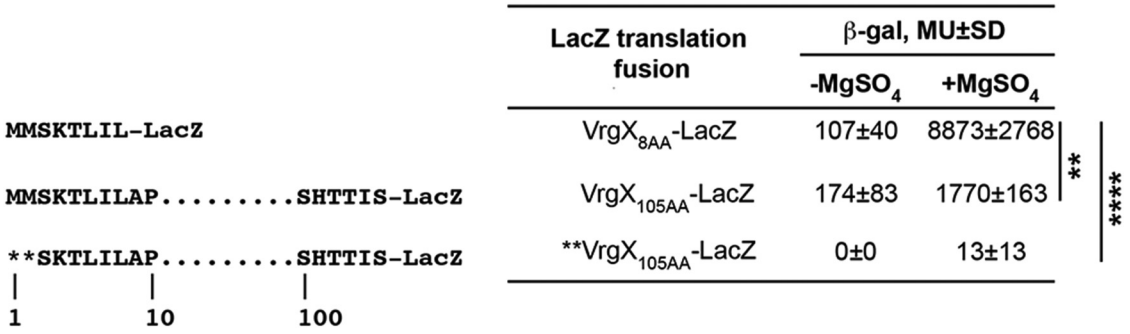

LacZ translation fusion	β-gal, MU±SD	
	-$MgSO_4$	+$MgSO_4$
$VrgX_{8AA}$-LacZ	107±40	8873±2768
$VrgX_{105AA}$-LacZ	174±83	1770±163
**$VrgX_{105AA}$-LacZ	0±0	13±13

, **

FIG 5 Translation of *vrgX-lacZ* in *B. pertussis*. Gene fragments coding for the $VrgX_{8AA}$, $VrgX_{105AA}$, and **$VrgX_{105AA}$ segments were cloned into the LacZ translation fusion vector pQC2123 and integrated *in situ* as a single copy in the chromosome of *B. pertussis* BP536. In **$VrgX_{105AA}$, the first two putative start codons, ATG (or Met), were replaced by TAG as indicated. The resulting *B. pertussis* strains were grown at 37°C for 48 h on BG agar in the presence or absence of 50 mM $MgSO_4$ and assayed for beta-galactosidase activity according to the method of Miller (38). Values are given in Miller units (MU). Data from at least three independent assays were used in the calculation of standard deviations (SD) and in statistical analysis using one-way ANOVA when $VrgX_{105AA}$ and **$VrgX_{105AA}$ were compared to the control, $VrgX_{8AA}$, in the presence of 50 mM $MgSO_4$. **, $P \leq 0.01$; ****, $P \leq 0.0001$.

BvgA∼P when $MgSO_4$ is present, as we have observed experimentally (15). As measured by these *lux* transcriptional fusions, in the Bvg^- mode, BRP-1304 exhibited very high activity, 261% of that of *vrg-73*. Taken together, these results demonstrate that BRP is a strong Bvg-repressed promoter that appears to be regulated by mechanisms that are similar to those regulating other *vrg*s.

The ORF downstream of BRP is translated *in vivo*. Analysis of sequences downstream of the BRP transcription start revealed an ORF, which we have named *vrgX*, which is preceded by a predicted Shine-Dalgarno sequence (AGGAG in Fig. 1) and separated from the first of two tandem ATGs by 8 bp. The *vrgX* gene is GC rich (70%) and extends into the P*fim3* promoter region, including the entire BvgA-binding region as well as the C stretch. As a result, coding of the C terminus of the hypothetical gene product VrgX will vary depending on the number of C residues in the C stretch. That number will dictate the reading frame 3′ to this feature, the amino acids encoded therein, and where the first stop codon is encountered. However, all three possible reading frames end before the start of the *fim3* ORF. These ORFs are illustrated in Fig. S5 as *vrgX*-13C for P*fim3*-13C, *vrgX*-14C for P*fim3*-14C, and *vrgX*-15C for P*fim3*-15C.

Because in earlier studies *vrgX* had not been recognized and annotated as an ORF, it has not been included in microarray studies and therefore was not previously identified as a *vrg* (30, 31). However, our recent RNA-seq analyses confirmed transcription of *vrgX* in the Bvg^- mode (32). To determine if *vrgX* was translated *in vivo*, we created an *in situ vrgX-lacZ* translational fusion in *B. pertussis* strain BP536 by cloning *vrgX* into the *lacZ* translation assay vector pQC2123 and integrating the resulting plasmid into *B. pertussis* in the same way as that for the *in situ* transcription assay vector pSS4162. As shown in Fig. 5, a fusion product containing the first 8 codons of *vrgX* fused to *lacZ* ($VrgX_{8AA}$-LacZ) was highly translated in the presence of $MgSO_4$ but not in the absence of $MgSO_4$, consistent with the *vrg*-like nature of BRP. To examine translation of a nearly full-length VrgX without the possible confounding effects of variation in the C stretch, we constructed this *vrgX-lacZ* fusion by fusing *lacZ* at a point just upstream of the C stretch ($VrgX_{105AA}$-LacZ) (Fig. 5). The $VrgX_{105AA}$-LacZ fusion also showed Bvg-repressed activity but at a level approximately 20% that of $VrgX_{8AA}$-LacZ (indicated by two asterisks in Fig. 5). To ensure that the translation detected in $VrgX_{105AA}$-LacZ was not caused by an internal translation restart within the *vrgX* ORF or the *lacZ* gene, we changed the tandem initial ATG codons of *vrgX* to amber mutant stop codons (TAGs) to generate a nonstart version of this fusion (designated **$VrgX_{105AA}$-LacZ). **$VrgX_{105AA}$-LacZ displayed very low levels of LacZ with or without $MgSO_4$ (indicated by four asterisks in Fig. 5), indicating that translational restarts within the *vrgX* gene are unlikely and that translation of this fusion protein initiates at the start codons of the *vrgX* ORF. Taken together, our results obtained from the *in vivo* translation fusion study

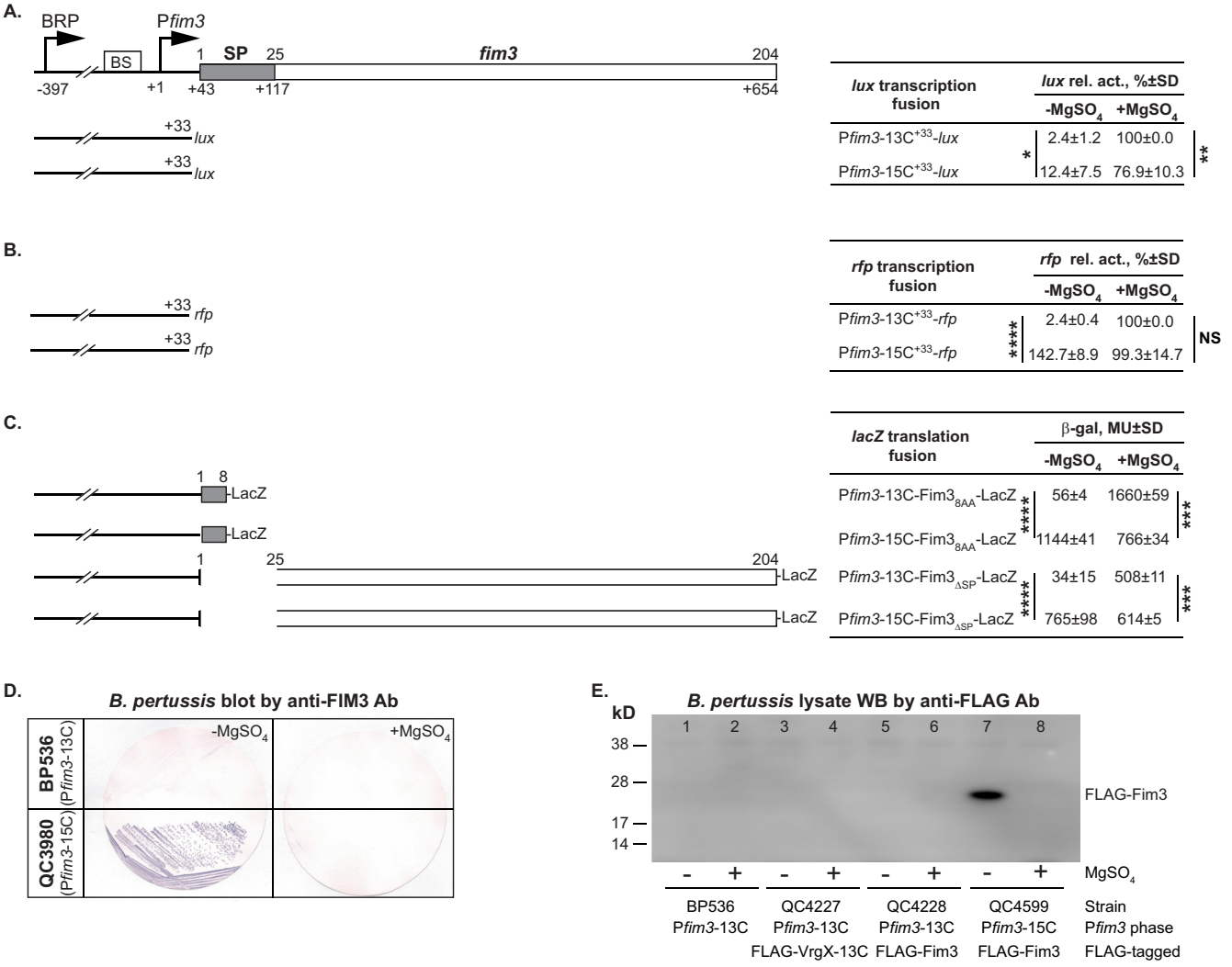

FIG 6 Transcription and translation of *fim3* in *B. pertussis*. (A and B) P*fim3* transcription assay *in situ*. The P*fim3* fragments were cloned into the *lux* transcription assay vector pSS4162 (A) or the *rfp* transcription assay vector pQC2319 (B) and integrated as a single copy *in situ* in the chromosome of *B. pertussis* strain BP536 P*fim3*-13C or QC3980 (P*fim3*-15C). The fusion points and other features for the cloned fragments are numbered relative to the P*fim3*-13C transcription start and presented schematically relative to the BRP-*fim3* region containing BRP, P*fim3*, BvgA binding sites (BS), signal peptide (SP), and *fim3* gene. The Fim3 amino acid numbers are indicated above the gray and white bars. Transcriptional activities are given as percent values, normalized to P*fim3*-13C^{+33} in the presence of 50 mM $MgSO_4$. rel. act., relative activity. (C) Demonstration of *fim3* translation. Fragments containing *fim3*$_{8AA}$ or *fim3*$_{\Delta SP}$ were cloned into the LacZ translation assay vector pQC2123 and integrated *in situ* in single copy in the chromosome of *B. pertussis* strain BP536 (P*fim3*-13C) or QC3980 (P*fim3*-15C). (A to C) Data from at least four assays were used to calculate the means and standard deviations (SD) and to conduct statistical analysis using unpaired two-tailed *t* test between two samples. NS, $P > 0.05$; *, $P \leq 0.05$; **, $P \leq 0.01$; ***, $P \leq 0.001$; ****, $P \leq 0.0001$. (D) Detection of FIM3 fimbriae by colony immunoblotting. Fimbria 3 production from the *B. pertussis* strains BP536 and QC3980 grown on BG agar in the absence or presence of 50 mM $MgSO_4$ was detected by colony immunoblotting using FIM3 monoclonal antibody (Ab). (E) Assay for Fim3 subunit and VrgX by Western blotting (WB). *B. pertussis* wild-type strain BP536 and its derivatives, QC4227, QC4228, and QC4599, which harbored FLAG fusions to VrgX or Fim3 grown in the absence (−) and presence (+) of 50 mM $MgSO_4$ at 37°C for 2 days, were collected and analyzed by SDS-PAGE followed by Western blotting using anti-FLAG M2 monoclonal antibody.

indicated that the BRP promotes the transcription and subsequent translation of its downstream gene, *vrgX*. However, it was unclear if this translation resulted in accumulation of a stable VrgX peptide.

To address this question, we used allelic exchange to modify the *vrgX* gene by placing sequences encoding a FLAG tag at the N terminus of VrgX (Fig. 1) in BP536, creating the strain QC4227 (BP536 FLAG–*vrgX*-13C). This strain was grown on BG agar, with and without $MgSO_4$, and whole-cell protein samples were electrophoresed and probed by Western blotting with anti-FLAG tag antibody. No band was detected in the Western blot that corresponded to the predicted size of FLAG–VrgX-13C, i.e., 14 kDa or 128 amino acids (aa) (Fig. 6E, lanes 3 and 4). As will be described in the following section, a similar construct for the *fim3* gene directed the expression of FLAG-Fim3 in

the absence of $MgSO_4$ (Fig. 6E, lane 7), demonstrating the general validity of this method. Taken together, these results indicate that transcription and translation of *vrgX* can occur *in vivo* but apparently do not lead to accumulation of VrgX peptide.

BRP directs transcription and translation of the Fim3 subunit. In light of the strong BRP-directed transcriptional readthrough into *fim3* (Fig. 2), we sought to determine if it could also result in Fim3 translation or the production of FIM3 fimbriae. To first quantify that readthrough, we used the *in situ* promoter-*lux* transcription fusion vector pSS4162 to measure transcriptional activity at a point downstream of the P*fim3* promoter (P*fim3*-13C^{+33}) in the Bvg$^-$ (with $MgSO_4$) mode and defined this level as 100% BRP activity. Activity in the Bvg$^+$ mode (without $MgSO_4$) was 2.4% of this value (Fig. 6A). Readthrough at the same point downstream of a permissive *fim3* promoter (P*fim3*-15C) in the Bvg$^-$ mode was 76.9%, indicating that the configuration of the C stretch had only a modest effect on readthrough from BRP (Fig. 6A and Fig. S6A). In the Bvg$^+$ mode, transcription in the P*fim3*-15C^{+33} context was increased to 12.4%, whereas 2.4% was observed in the P*fim3*-13C^{+33} context. This increased transcription of P*fim3*-15C^{+33} in the Bvg$^+$ mode presumably represented activity of a functional P*fim3* promoter and thus is consistent with previously observed differences in activity between the permissive and nonpermissive states of P*fim3* when examined ectopically (13).

It should also be noted that transcription from P*fim3*-15C^{+33}, although higher than that from P*fim3*-13C^{+33}, was still much weaker than that from the similar *fim2* promoter in a permissive configuration (P*fim2*-12C^{-32}), as observed previously (13). A previous study to determine the bases of this discrepancy revealed the presence of a 15-bp repressive element (DRE), immediately downstream of P*fim3* +1, that reduced the *in vivo* level of transcription from P*fim3* by more than 200-fold, as measured by *lux* transcriptional fusions (34). In this study, we have also used *rfp* as a reporter gene. This was accomplished by replacing *luxCDABE* in pSS4162 with a gene for a red fluorescent protein, *rfp*. We used the resulting vector to create *in situ* fusions at the same points as those of *lux* shown in Fig. 6A, yielding the results shown in Fig. 6B and Fig. S6B. Transcriptional activity of P*fim3*-13C^{+33}-*rfp* in the Bvg$^-$ mode (with $MgSO_4$), representing BRP activity, was significant, confirming readthrough from BRP, and was set as 100%. Activity in the Bvg$^+$ mode (without $MgSO_4$) was only 2.4% of that. For P*fim3*-15C^{+33}-*rfp*, activity in the Bvg$^-$ mode (with $MgSO_4$) was similar to that for P*fim3*-13C^{+33}-*rfp*, indicating again that the state of the *fim3* promoter did not affect BRP readthrough. However, activity in the Bvg$^+$ mode (without $MgSO_4$), representing transcription originating downstream of P*fim3*-15C^{+33}, was more than 10-fold higher than that when measured with a *lux* fusion. We conclude on the basis of these new data that the DRE effect we reported previously may in fact be specific to the *luxCDABE* fusion partner, and that this type of fusion may not be an accurate reporter of transcriptional activity in some genetic contexts. Thus, the DRE does not appear to limit *fim3* transcription from P*fim3* in its native genetic context. However, it should be noted that, for reasons that are currently not understood, the DRE effect does depend on the host strain, as it was observed in bordetellae but not in *Escherichia coli* (34). Nevertheless, *vrg*-like transcription of the *fim3* gene, promoted by BRP in the Bvg$^-$ mode and independent of the state of the P*fim3* promoter, has now been confirmed using two different types of *in situ* transcriptional gene fusion. The presence of the BRP therefore provides an explanation for previous observations from transcriptional profiling studies indicating that *fim3* behaved as a *vrg* (30–32).

To determine whether transcription from BRP could result in translation of the *fim3* gene, we created *in situ* translational fusions of LacZ to the first 8 amino acids of Fim3 in the context of P*fim3*-13C in BP536 to obtain P*fim3*-13C-Fim3$_{8AA}$-LacZ and of P*fim3*-15C in QC3980 to obtain P*fim3*-15C-Fim3$_{8AA}$-LacZ. As presented in Fig. 6C, BRP-promoted expression of these fusions was observed in both constructs in the presence of $MgSO_4$, whereas in the absence of $MgSO_4$, Bvg-dependent expression was observed

only if P*fim3* was in a permissive configuration (P*fim3*-15C-Fim3$_{8AA}$-LacZ). To determine whether BRP-initiated transcription of *fim3* extended through the entire gene, we created full-length LacZ translational fusions to the end of the *fim3* ORF from which the 24-aa signal peptide (35) was deleted (Fim3$_{\Delta SP}$) to allow cytoplasmic localization of the fusion protein in order to avoid toxicity from secretion of the LacZ moiety. Although LacZ activity from these fusions was somewhat reduced relative to that from the 8-aa derivatives, translation clearly extended to the end of the *fim3* gene (Fig. 6C).

Expression of *fim3* from BRP does not result in the production of FIM3 fimbriae. Since we observed translation of *fim3* under the control of BRP in the Bvg$^-$ mode, we sought to investigate whether BRP activity under these conditions also led to the production of FIM3 fimbriae. Using a monoclonal antibody against FIM3 fimbriae to probe a colony immunoblot of *B. pertussis* grown on BG agar, fimbria production was detected only in strain QC3980 (P*fim3*-15C) without $MgSO_4$ (Fig. 6D). Either the presence of $MgSO_4$ or a nonpermissive configuration (P*fim3*-13C) led to a lack of extracellular fimbriae detectable by this antibody. Even though the results presented in the previous section indicated that the *fim3* gene could be transcribed and translated in the presence of $MgSO_4$ (Bvg$^-$ mode), the *fimBCD* genes encoding the fimbrial chaperone, usher, and tip adhesin proteins are not, being encoded within the Bvg-regulated *fha* operon.

To more clearly understand the fate of the Fim3 subunit expressed in the Bvg$^-$ mode, we engineered two strains in which a FLAG tag was present between D27 and G28 of Fim3, i.e., after the signal peptide but at the N terminus of the processed protein (Fig. 1). In strain QC4228 FLAG-Fim3 is under the control of P*fim3*-13C and in strain QC4599, FLAG-Fim3 is under the control of P*fim3*-15C. Whole-cell protein samples from both strains, grown in the presence and absence of $MgSO_4$, were electrophoresed and Western blotted with anti-FLAG antibody to detect FLAG-Fim3. As shown in Fig. 6E, lane 7, FLAG-Fim3 was detected only in samples from QC4599 grown in the absence of $MgSO_4$, i.e., under the control of an active P*fim3* in the Bvg$^+$ mode. It should also be noted that, in QC4599 in the Bvg$^+$ mode, the FLAG-Fim3 protein was properly assembled into fimbriae and to the same level as that in QC3980 (Fig. 6D), as detected by colony Western blotting with antibody against Fim3 fimbriae (data not shown). The lack of detectable FLAG-Fim3 in QC4599 grown in the presence of $MgSO_4$ suggests that even though translation of *fim3* occurs in the Bvg$^-$ mode, promoted by BRP, Fim3 protein does not accumulate. We propose that cytoplasmic Fim3 protein, in the absence of the molecular machinery to export and assemble it, is unstable and therefore not detected.

Transcriptional profiles of *fim2*, *fim3*, and *vrgX* in *B. pertussis*. To more definitively establish BRP-directed expression of the *fim3* gene, under native conditions and without the use of gene fusions, we also assessed transcription of key genes by measuring RNA levels directly. To this end, we used reverse transcription-quantitative PCR (RT-qPCR) to monitor the expression of *fim2*, *fim3*, and *vrgX* in the wild-type *B. pertussis* strain BP536 carrying P*fim*-13C and in the strain QC3980 carrying P*fim*3-15C. As expected and consistent with previous transcriptional profiling studies (30–32), in BP536 the *fim*3 gene was transcribed only in the Bvg$^-$ mode (with $MgSO_4$), displaying a *vrg*-like behavior, and the Bvg-activated *fim*2 gene was expressed only in the Bvg$^+$ mode (without $MgSO_4$) (Fig. 7). The expression of *vrgX* was very similar to that of *fim3* in BP536, as it also represents transcription from BRP, which, as we now understand, is the root cause of *fim3 vrg*-like behavior. However, a high level of *fim3* transcription was detected in the Bvg$^+$ mode (without $MgSO_4$) in strain QC3980 in which the P*fim*3-15C is in an on state, consistent with previous work from our group and others (11, 13). As expected, the permissive state of *Pfim3* had no effect on BRP-directed transcription of *vrgX* and *fim3* in the Bvg$^-$ mode.

BRP transcriptional readthrough is impaired by the downstream 62-bp GC-rich region in *B. bronchiseptica*. A comparison of the genomic DNA sequences of *B. pertussis* BP536 and *B. bronchiseptica* RB50 in the vicinity of BRP reveals that although the core BRP is identical between the two species, a 62-bp segment of very high GC

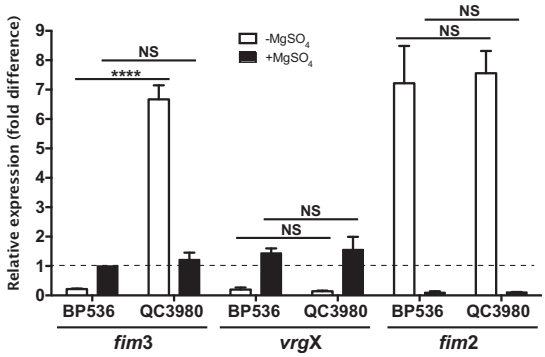

FIG 7 Quantitative PCR of *in vivo fim2*, *fim3*, and *vrgX* expression. RNA prepared from *B. pertussis* strains BP536 (P*fim3*-13C) and QC3980 (P*fim3*-15C) grown on BG agar in the absence (white bar) or presence (black bar) of 50 mM $MgSO_4$ was reverse transcribed to cDNA, followed by qPCR analysis of genes *fim2*, *fim3*, and *vrgX*. Expression levels, after normalization to the *rpoD* gene, used as an internal control, are given as fold difference relative to *fim3* expression in BP536 in the presence of $MgSO_4$. The mean values and standard deviations, in error bars, were calculated from three biologically independent determinations and used to conduct statistical analysis using unpaired two-tailed *t* test between two samples. NS, $P > 0.05$; ****, $P \leq 0.0001$.

content (87%) is absent from *B. pertussis* that is present in *B. bronchiseptica*. No obvious sequence signatures are present at the boundaries of this polymorphism that would suggest a directed mechanism of insertion in *B. bronchiseptica* or deletion in *B. pertussis*. Therefore, we conclude that this feature represents a spontaneous deletion that occurred on the evolutionary path to *B. pertussis*. The endpoints of this deletion are within the *vrgX* ORF, which is present as a result. To determine the possible effects of this polymorphism on transcription of downstream genes, we assessed promoter activity from a *B. bronchiseptica* BRP fragment that had limits identical to those of the BRP-1304 fragment we have used to study BRP from *B. pertussis*. This fragment, BRP-1770 (Fig. S3), was then similarly cloned into plasmid pSS3967 and integrated into wild-type *B. pertussis* BP536 at the ectopic location. Under modulating conditions (with $MgSO_4$) in strain BP536, BRP-1770 displayed only 9% of the activity observed with BRP-1304 (Fig. 8), indicating that the 62-bp region with high GC impeded BRP transcriptional readthrough. This observation thus explains the lack of anomalous *fim3* transcription in *B. bronchiseptica* (36).

DISCUSSION

Production of the extracellular adhesion organelles known as fimbriae is regulated in *B. pertussis* at multiple levels. Belonging to the chaperone-usher family of fimbrial

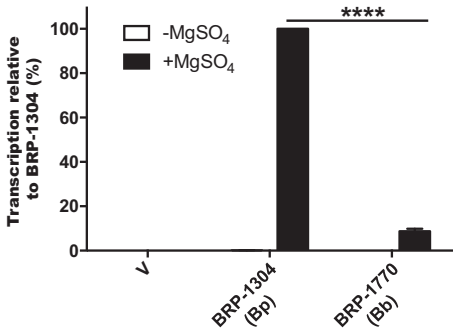

FIG 8 Ectopic transcription of BRP-1304 (Bp) and BRP-1770 (Bb) in *B. pertussis*. The wild-type *B. pertussis* strain BP536, carrying various ectopically integrated pSS3967-based ectopic promoter-*lux* fusions, empty vector pSS3967 (V), pQC-BRP-1304 [BRP-1304 (Bp)], and pQC-BRP-1770 [BRP-1770 (Bb)], described in Fig. S3, were grown on BG agar at 37°C for 2 days in the absence or presence of 50 mM $MgSO_4$ and analyzed for light output by luciferase as described in Materials and Methods. Activity measurements are presented relative to that in the BP536 strain carrying BRP-1304 (Bp) and represent the averages from at least four assays, with error bars indicating the standard deviations. Statistical analysis by unpaired two-tailed *t* test was conducted. ****, $P \leq 0.0001$.

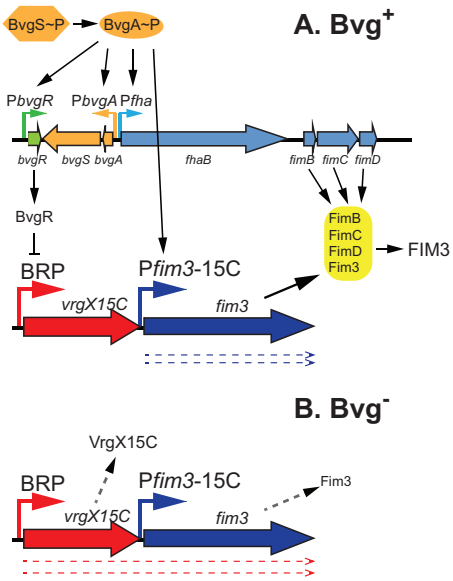

FIG 9 Model of FIM3 fimbrial regulation in *B. pertussis*. (A) In the Bvg$^+$ mode, the BvgAS two-component system directly activates transcription of multiple virulence promoters, such as P*bvgR*, P*bvgA*, P*fhaB*, and P*fim3* (active with a stretch of 15 C residues but inactive with a stretch of 13 C residues). Fim3 subunit proteins are further assembled into fully functional surface-exposed fimbriae FIM3 in the presence of fimbrial accessory proteins FimB, FimC, and FimD, whose genes are under the control of P*fha*. The BRP is not activated due to the presence of BvgR. (B) In the Bvg$^-$ mode, induced by $MgSO_4$, Bvg-activated genes are silenced and the Bvg-repressed genes, including BRP, are expressed under the control of the activator RisA (not shown). Although BRP directs the transcription and subsequent translation of *vrgX* and the downstream *fim3*, the products of the genes are not stable (indicated by the dashed lines). For Fim3 this is due to the lack of other gene products needed for fimbria production.

biogenesis systems, the chaperone, usher, and tip adhesin genes, *fimB*, *fimC*, and *fimD*, respectively, are located within the *fha* operon, which also includes the genes for filamentous hemagglutinin (FHA) and its accessory proteins. They are therefore regulated by the virulence master regulatory two-component system, *bvgAS*. However, the genes for different serotypes of major fimbrial subunits are located at unlinked locations. The expression of these genes, *fim2*, *fim3*, and *fimX*, is directly regulated by binding of BvgA~P (13), but they also are regulated individually in a phase-variable fashion (11). The latter occurs through variation in the length of a monotonic stretch of C residues within the *fim* promoters, with a permissive configuration allowing proper spatial relationships between bound BvgA~P and RNA polymerase and a nonpermissive configuration preventing those relationships (13). In this study, we characterize yet another aspect of regulation of one *fim* gene, *fim3*, and show that expression of *fim3* is also driven by readthrough transcription from a newly discovered promoter upstream of the BvgAS-regulated P*fim3* that we have called BRP, for Bvg-repressed promoter.

As its name implies, BRP activity is regulated inversely to that of Bvg-activated genes (*fim*s and other virulence factors) and is therefore a member of the *vrg*s, or *vir*-repressed genes. In addition, as we show here, its regulation is mechanistically similar to that of other previously described *vrg*s, in that it requires the response regulator RisA for expression (27–29) and exhibits constitutive activity in a *bvgA* or *bvgR* mutant, the latter being a negative regulator of *vrg* expression (17, 18). As depicted in Fig. 9, the discovery of the BRP provides an explanation for the *vrg*-like behavior of *fim3* in transcriptomic analyses (30–32). Such behavior is at odds with expression of FIM3 fimbriae as a Bvg-activated trait, as well as the observation that isolated P*fim3* behaves as a *vag in vivo* and that transcription from P*fim3* is activated *in vitro* by BvgA~P (11, 13).

Not unexpectedly, BRP-mediated transcription of *fim3* extends to the end of the *fim3* ORF (data not shown). Using translational gene fusions to LacZ, we showed that

transcripts originating at BRP (in the Bvg$^-$ mode) can in fact support translational initiation of Fim3 as well, and that translation can extend all the way through the *fim3* gene. However, Western blot analysis of Fim3 provided with a FLAG tag did not reveal any accumulation of Fim3 protein under these conditions. It should be noted that a tag such as FLAG had to be used because antisera to FIM3 fimbriae currently available have been raised against assembled fimbriae and do not detect the monomeric Fim3 in Western blotting. Despite considerable effort, we have been unable to generate antibodies that do. In contrast to what we observed in the Bvg$^-$ mode, in the Bvg$^+$ mode, if the *fim3* promoter was in a permissive state, extracellular FIM3 fimbriae were detectable by colony immunoblot and the FLAG-tagged Fim3 protein was detectable by Western blotting. This is not surprising, because in the Bvg$^+$ mode the FimBCD proteins, required for export and assembly of complete fimbriae, are also expressed. A straightforward hypothesis for the lack of Fim3 accumulation in the Bvg$^-$ mode is that unassembled Fim3 protein in the cytoplasm is unstable (Fig. 8). However, this begs the question, what is the evolved role of BRP? Is it to express another gene?

Just downstream of BRP and upstream of P*fim3*, in *B. pertussis*, resides an ORF that we have called *vrgX*. The predicted peptide encoded shows no amino acid sequence similarity to any protein in the GenBank database. This ORF is preceded by an excellent ribosome binding site (AGGAG in Fig. 1), and our data using translational gene fusions indicate that it is also translated under Bvg$^-$ conditions. However, as with the *fim3* gene, this translation does not result in the accumulation of detectable VrgX protein (Fig. 6E). Our efforts to date, including whole-genome transcriptomic analysis by microarray, to associate integrity, or the lack thereof, of this ORF with any detectable phenotype have failed. However, in thinking about a role for BRP, it may be worthwhile comparing the context of BRP in *B. pertussis* to that in *B. bronchiseptica*, illustrated in Fig. 1. Phylogenetic analyses indicate that *B. pertussis* and *B. bronchiseptica* diverged relatively recently from a common ancestor that was similar to *B. bronchiseptica* (33). Thus, an evolved function for BRP might be expected to be more discernible in the latter species. This is especially true since although the DNA sequence of the core BRP is identical in the two species, the region downstream is different (Fig. 1; see also Fig. S3 in the supplemental material). In this region, within a segment of very high GC content, there is a deletion of 62 bp in *B. pertussis* relative to *B. bronchiseptica*. This deletion has two consequences. One is the creation of the *vrgX* ORF, present in *B. pertussis* but not in *B. bronchiseptica*. The other, functional, difference is that transcription from BRP can extend more efficiently into *fim3*. The evidence for this, reported here, is that deletion of this 62-bp segment from the wild-type *B. bronchiseptica* RB50 BRP region results in increased transcription downstream. Although exactly how this 62-bp segment causes transcriptional attenuation is unknown, its high GC content suggests the possibility of extended RNA secondary structure. It is conceivable that either the presence of the "new" *vrgX* ORF or increased transcriptional readthrough could have led to a selective advantage for a *B. pertussis* evolutionary intermediate.

Evolution of inverse expression of the genes recognized as *vrg*s in *B. pertussis* (including BRP-*vrgX*) apparently also occurred after the split between the *B. pertussis* and *B. bronchiseptica* lineages and is the subject of ongoing investigation. One scenario for this would be as follows. *B. pertussis*, in the process of evolving from a chronic, multihost pathogen like *B. bronchiseptica* to a human-restricted acute pathogen, experienced a selectable advantage due to activation of the *vrg*s in a Bvg-repressed fashion. In fact, recent studies have suggested that expression of this arm of the Bvg regulon in *B. pertussis* does in fact lead to increased survival in static aerosols and to increased aerosol transmission to naive baboons (T. Merkel, unpublished data). In addition, recent transcriptome analyses have revealed that multiple genes, for varied metabolic pathways that are associated with bacterial survival, transmission, and/or persistence, are significantly upregulated in the *B. pertussis* Bvg$^-$ mode (32). Activation of the *vrg*s would have included activation of BRP, possibly impacting *B. pertussis* survival negatively, due to high levels of expression of the BRP transcript. This RNA might have had regulatory roles of its own, perhaps due to extended secondary

structure as a result of its high GC content. Thus, there might have been selection for the inactivation of this RNA effector, leading to the deletion observed today in *B. pertussis*. If this reasoning is correct, the creation of the *vrgX* ORF may have been an unselected consequence of the deletion. On the other hand, it may be that it was the creation of the *vrgX* ORF, rather than the loss of the GC-rich region, that led to a selective advantage for the evolving *B. pertussis* evolutionary intermediate.

Clearly more work will be required to understand the functions of BRP and *vrgX* in the natural history of *B. pertussis* and *B. bronchiseptica*. However, for the time being, BRP is an extremely valuable tool with which to decipher the mechanistic bases of regulation of all the Bvg-repressed genes, as demonstrated in recent studies (29).

MATERIALS AND METHODS

Bacterial strains and culture conditions. Bacterial strains and plasmids used in this study are listed in Table 1, and primers are listed in Table S1 in the supplemental material. *E. coli* strains were grown in LB broth or on LB agar. Antibiotic concentrations used in LB for *E. coli* strains were 100 μg/ml ampicillin and 5 μg/ml gentamicin. *B. pertussis* strains were grown on BG agar (37). Antibiotic concentrations used in BG agar for *B. pertussis* strains were the following: streptomycin, 50 μg/ml; spectinomycin, 50 μg/ml; gentamicin, 10 μg/ml or 100 μg/ml, as indicated. To support the growth of *E. coli* strain RHO3, 200 μg/ml of 2,6-diaminopimelic acid (DAP; Alfa Acesar, UK) was used in LB broth, in LB agar, or in BG agar.

Construction of plasmids and strains is described in the supplemental materials and methods.

***In vivo* luciferase and RFP activity assays.** *B. pertussis* strains harboring promoter-*lux* fusions in pSS3967 and pSS4162 (Fig. S1) or promoter-*rfp* fusions in pQC2319 (Fig. S7B) were streaked in sectors on BG agar containing streptomycin and gentamicin and grown for 48 h at 37°C. When desired, to modulate BvgAS-mediated regulation in *B. pertussis*, 50 mM $MgSO_4$ was included in the BG agar. Light output was detected and imaged using an IVIS-50 instrument (Caliper Life Sciences). For quantitative determination, the total flux (photons per second) of a circular region of interest (ROI) of 0.5-cm diameter in the middle of each sector was derived using Living Image software, V4.4 (Caliper Life Sciences), as described previously (13). Data, averaged from at least 4 assays, were presented as arbitrary relative luminescence units (RLU; photons per second) or fluorescence units (RFU) or are relative to the wild-type promoter control strain or other luminescent or fluorescent strains used as a reference on a given plate.

β-Galactosidase assay. *B. pertussis* strains harboring *lacZ* fusions in pQC2123 (Fig. S7A) were streaked in sectors and grown at 37°C for 48 h on BG agar containing streptomycin and gentamicin in the presence or absence of 50 mM $MgSO_4$. Bacteria to be assayed were recovered by placing a sterile Dacron swab into 1.5 ml of Tris-HCl, pH 8.0. After measurement of A_{600}, 50 μl of the cell suspension was added to 0.95 ml Z-buffer and assayed as described by Miller (38).

Primer extension and transcriptional start determination. *B. pertussis* strains BP536 and QC3980 were grown for 2 days in either the presence or absence of 50 mM $MgSO_4$ on BG agar containing streptomycin or, in the case of BP536 harboring the *lux* fusions BRP-1339 and BRP-1340, streptomycin and gentamicin. Cells were collected by swabbing and resuspended in 3 ml of phosphate-buffered saline (PBS). After centrifugation at 2,600 $\times$ *g* for 15 min, cell pellets were resuspended in 1 ml PBS and transferred to 1.5-ml microcentrifuge tubes. Cell pellets obtained after centrifugation at 14,000 $\times$ *g* for 1 min were stored at −80°C.

RNA was isolated by Hinton method II (39). Primer extension analyses were performed as described previously (40, 41) using AMV reverse transcriptase (Life Sciences, Inc.), 1 μg of the indicated RNA (as measured by A_{260}), and oligodeoxyribonucleotide primers that were 5′ ^{32}P end labeled using [γ-^{32}P]ATP and Optikinase (USB). Primer sequences are given in Fig. 1 (primer 77-57) and in Fig. 3 (primers 1340 and BRE-2). Cold P*tac* RNA, used as control RNA in some reaction mixtures, was generated *in vitro* using the plasmid pGEX-5X-3 DNA (Pharmacia Biotech), which contains the P*tac* promoter. Transcription reaction mixtures were as described previously (42), except that the concentration of each ribonucleoside triphosphate was 200 μM and no labeled ribonucleoside triphosphate was added. The 5′ ^{32}P-labeled P*tac* primer (5′CCAATAACCTAGTATAG) anneals 66 nt from the start of the P*tac* RNA and yields a set of products (43). The 5′ ^{32}P-labeled primer BRE-2 was also used for dideoxy sequencing (44), using the plasmid pQC1340, containing the BRP-1340 fragment as a template. Sequencing ladders that were so generated were electrophoresed alongside primer extension reactions and, in some lanes, were doped with the primer extension product to allow precise localization of the initiation nucleotide.

Primer extension products were separated on 7 M urea–5% acrylamide polyacrylamide gels. After autoradiography, films were scanned using a Powerlook 100XL densitometer (Bio-Rad).

Colony immunoblotting. *B. pertussis* strains BP536 and QC3980 were grown for 2 days either in the presence or absence of $MgSO_4$ (50 mM) on BG agar containing streptomycin. An 82-mm-diameter circular nitrocellulose filter (Schlecher & Schuell) was laid onto the agar surface until the filter was fully wetted and then removed along with adherent colonies. The filter was washed and blocked by laying it, colony side up, onto the surface of approximately 30 ml PBS-T (phosphate-buffered saline [pH 7.2], 0.05% Tween 20) containing 1% bovine serum albumin (BSA), followed by agitation by rotation to remove bacterial growth. This step was repeated until the wash was no longer turbid with bacterial cells, and the blot was further blocked by incubation in PBS-T plus BSA for 1 h, followed by 3 washes for 5 min each in PBS-T. Incubation with anti-fimbria 3 monoclonal antibody (laboratory collection) was in a 1:1,000 dilution in 1% BSA in PBS-T at room temperature for 1 h. After the filter was washed three times with PBS-T for 10 min each time, it was incubated

TABLE 1 Bacterial strains and plasmid used in this study

Strain or plasmid	Relevant feature(s)	Source or reference
E. coli		
DH5α	High-efficiency transformation	Bethesda Research Laboratories
SM10	Mobilization of RK2 *oriT* plasmids	45
RHO3	SM10(*λpir*) Δ*asd*::*FRT* Δ*aphA*::*FRT*	46
B. pertussis		
Tohama I	Patient isolate, P*fim3*-13C	47
BP536	Tohama I Str^r Nal^r P*fim3*-13C	37
BP1526	BP536 Δ*bvgA*	13
TM1793	BP536 Δ*bvgR*	27
TM1627	BP536 Δ*risA*	27
QC3818	BP536 ΔBRP-*fim3*::P*pol phoA* Spc^r	This study
QC3980	BP536 P*fim3*-15C	This study
QC4227	BP536 FLAG-*vrgX*-13C	This study
QC4228	BP536 P*fim3*-13C-FLAG-*fim3*	This study
QC4599	BP536 P*fim3*-15C-FLAG-*fim3*	This study
Plasmids		
pGEX-5X-3	P*tac* promoter, Amp^r	Pharmacia Biotech
pSS3967	Ectopic *luxCDABE* promoter assay vector, Amp^r Gen^r	13
pQC1557	pSS3967::P*fhaB*	34
pQC1646	pSS3967::*vrg-6* (2610863 to 2612172 of *B. pertussis* Tohama I)	29
pQC1647	pSS3967::*vrg-18* (910232 to 911273 of *B. pertussis* Tohama I)	29
pQC1648	pSS3967::*vrg-24* (3713213 to 3713862 of *B. pertussis* Tohama I)	29
pQC1649	pSS3967::*vrg-73* (3494967 to 3495955 of *B. pertussis* Tohama I)	29
pQC1304	pSS3967::BRP-1304 (1646945 to 1647500 of *B. pertussis* Tohama I)	29
pQC-BRP-N	pSS3967::BRP-N[a]	This study
pSS4162	*In situ luxCDABE* promoter assay vector, Amp^r Gen^r	This study
pQC1069	pSS4162::P*fim2*-12C^{+32} (1177502 to 1176483 of *B. pertussis* Tohama I) (P*fim2*-12C, −988 to +32)	This study
pSS4276	pSS4162::P*fim3*-13C^{+33} (1646615 to 1647592 of *B. pertussis* Tohama I) (P*fim3*-13C, −945 to +33)	This study
pSS4278	pSS4276 P*fim3*-15C	This study
pQC1282	pSS4162::P*fim3*-13C^{-60} (P*fim3*-13C, −1560 to −60)	This study
pQC1283	pSS4162::P*fim3*-13C^{-616} (P*fim3*-13C, −1560 to −616)	This study
pQC2123	*In situ lacZYA* translation assay vector, Amp^r Gen^r	This study
pQC2125	pQC2123::VrgX$_{8AA}$-LacZ	This study
pQC2126	pQC2123::VrgX$_{105AA}$-LacZ	This study
pQC2264	pQC2123::**VrgX$_{105AA}$-LacZ	
pQC2180	pQC2123::P*fim3*-13C-Fim3$_{8AA}$-LacZ	This study
pQC2182	pQC2123::P*fim3*-13C-Fim3$_{\Delta SP}$-LacZ	This study
pQC2186	pQC2123::P*fim3*-15C-Fim3$_{8AA}$-LacZ	This study
pQC2188	pQC2123::P*fim3*-15C-Fim3$_{\Delta SP}$-LacZ	This study
pQC1883	*B. pertussis* inducible protein expression vector, Kan^r	15
pQC2113	pQC1883::*rfp* Kan^r	This study
pQC2240	pQC2123 Δ*lacZYA rfp* Amp^r Gen^r	This study
pQC2319	*In situ rfp* promoter assay vector, Amp^r Gen^r	This study
pQC2309	pQC2319::P*fim2*-12C^{+32}-*rfp*	This study
pQC2310	pQC2319::P*fim3*-13C^{+33}-*rfp*	This study
pQC2311	pQC2319::P*fim3*-15C^{+33}-*rfp*	This study
pSS4894	Allelic exchange vector P*ptx*-I-SceI, I-SceI site, *oriT* Gen^r	29
pQC2076	pSS4894::BRP-*fim3* (−950 to +1255) Δ−349 to +656, Gen^r	This study
pQC2077	pQC2076::I-*PpoI* site, Spc^r-*phoA* at deletion site, Gen^r Spc^r	This study
pUC57	Cloning vector, Amp^r	Genscript
pQC2078	pUC57::BRP-*fim3* region (−357 to +664) (P*fim3*-13C), Amp^r	This study
pQC2094	pQC2078 P*fim3*-15C Amp^r	This study
pQC2197	pQC2078 FLAG-*vrgX* Amp^r	This study
pQC2199	pQC2078 FLAG-*fim3* Amp^r	This study
pQC2322	pQC2094 FLAG-*fim3* Amp^r	This study
pQC2095	pSS4894::P*fim3*-15C (−950 to +1255) Gen^r	This study
pQC2198	pSS4894::FLAG-*vrgX* (−950 to +1255) Gen^r	This study
pQC2200	pSS4894::P*fim3*-13C-FLAG-*fim3* (−950 to +1255) Gen^r	This study
pQC2323	pSS4894::P*fim3*-15C-FLAG-*fim3* (−950 to +1255) Gen^r	This study

[a]In BRP-N, N refers to the BRP fragment indicated in Fig. S3 and S4.

with goat anti-mouse Ig (H+L) conjugated with alkaline phosphatase (Southern Biotechnology Associated, Inc.) at a 1:5,000 dilution in 1% BSA in PBS-T at room temperature for 1 h. The filter was then washed with PBS-T for 10 min, three times, and rinsed with AP buffer (100 mM Tris-HCl, 100 mM NaCl, 5 mM $MgCl_2$, pH 9.5) for 5 min. To visualize the alkaline phosphatase activity, the filter was incubated with 5 ml AP buffer containing 33 μl nitroblue tetrazolium (50 mg/ml; Promega) and 16.5 μl 5-bromo-4-chloro-3-indolylphosphate (50 mg/ml; Promega) and stopped after the desired color had developed by transfer to TE buffer (10 mM Tris-HCl containing 1 mM EDTA, pH 8.0).

SDS-PAGE and Western blotting. *B. pertussis* strains QC4227 (BP536 FLAG–*vrgX*-13C), QC4228 (BP536 P*fim3*-13C FLAG-*fim3*), and QC4599 (BP536 P*fim3*-15C FLAG-*fim3*) were grown at 37°C for 2 days on BG agar plus streptomycin with or without 50 mM $MgSO_4$. To prepare cell lysates for SDS-PAGE, cells were swabbed from the plate with a polyester-tipped applicator (Puritan Medical Products Company, LLC) and resuspended in 1 ml of PBS (Gibco) to an optical density at 600 nm (OD_{600}) of 1.0. To collect all of the proteins, including those in the supernatant, 0.25 ml of 100% (wt/vol) trichloroacetic acid (TCA) was added, and the cell suspension, at a final TCA concentration of 20%, was incubated on ice for 20 min. After centrifugation at 15,000 $\times$ *g* for 15 min at 4°C, the pellets were resuspended in 100 μl of 1$\times$ NuPAGE SDS sample buffer (Invitrogen) and boiled for 5 min. Ten microliters of each treated sample was loaded on a NuPAGE 4 to 12% Bis-Tris gel (Invitrogen). Electrophoresis was performed at 150 V for 80 min using NuPAGE MES SDS running buffer (Invitrogen). Transfer of the gel to a polyvinylidene difluoride (PVDF) filter (Invitrogen) was carried out using the Mini-PROTEAN II (Bio-Rad) apparatus at a constant voltage of 100 V for 1 h with ice cooling. After removal from the transfer apparatus, the PVDF filter was blocked overnight with 5% nonfat milk in PBS, washed with PBS, and then incubated with anti-FLAG M2 monoclonal antibody (Sigma) diluted 1:1,000 in PBS containing 1% nonfat milk for 1 h, followed by three washes (15 min each) with PBS-T. The filter was then incubated with goat anti-mouse IgG–horseradish peroxidase conjugate (Santa Cruz) at a 1:20,000 dilution in PBS containing 1% milk at room temperature for 1 h. After three washes (15 min each) with PBS plus 0.05% Tween, the filter was developed using the Amersham ECL plus Western blotting detection system (GE Healthcare) and imaged using a G:Box imaging system (Syngene).

RT-qPCR analysis. To prepare RNA, *B. pertussis* strains BP536 and QC3980 were grown for 2 days either in the presence or absence of $MgSO_4$ (50 mM) on BG agar containing streptomycin. The cells from approximately half of a plate of culture were collected using a polyester swab and resuspended in 6 ml of stabilization mix, obtained by mixing 1 volume of PBS and 2 volumes of RNAprotect bacterial reagent (Qiagen). For each sample, the resuspended cells representing 2 OD_{600} units were pelleted in a microcentrifuge at 15,000 $\times$ *g* for 2 min at room temperature and then resuspended in 150 μl TE buffer supplemented with 0.5 mg lysozyme (MP Biomedicals). After incubation at room temperature for 10 min on a shaking platform, 525 μl RLT buffer (Qiagen) containing 2-mercaptoethanol at 10 μl/ml was added to the partially lysed cells and vortexed immediately for 5 s. To further lyse the cells, the suspension was transferred to FastRNA blue tubes (2 ml; MP Biomedicals) and processed in a FastPrep bead beater (MP Biomedicals) for 45 s at a setting of 6.5. The supernatants (~400 μl), after centrifugation at 15,000 $\times$ *g* for 5 min at 4°C, were then transferred to 2-ml microcentrifuge tubes containing 280 μl of 100% ethanol (0.7 volume) and processed with a QIAcube (Qiagen) using the program RNeasy Protect Bacteria. The RNA sample was obtained in a 50-μl volume and was further treated with DNase using the Turbo DNA-free kit (Ambion), followed by quality and quantity assessment using Quant-iT PicoGreen double-stranded DNA assay (Invitrogen), NanoDrop analysis (NanoDrop Technologis), and Bioanalyzer analysis (Agilent).

For cDNA synthesis, 1 μg of high-quality RNA in a total of 9 μl of nuclease-free water was supplemented with 4 μl of 10 mM deoxynucleoside triphosphate mixture and 1 μl of random primers (250 ng/ml; Invitrogen) and then denatured at 65°C for 10 min, followed by cooling on ice. Each denatured RNA sample was further supplemented with 4 μl 5$\times$ buffer, 1 μl 0.1 M dithiothreitol, 1 μl SuperScript III reverse transcriptase (Invitrogen), and 1 μl RNaseOUT recombinant RNase inhibitor (Invitrogen). Primers were allowed to anneal at room temperature for 5 min, followed by the reverse transcription reaction at 50°C for 60 min, followed by a final 15-min enzyme denaturation step at 70°C for 15 min. Removal of RNA was performed using 1 μl of *E. coli* RNase H for 20 min at 37°C. For each sample, the same reaction without reverse transcriptase was also assembled as a control for DNA contamination.

RT-qPCR was performed using the CFX connect real-time system (Bio-Rad). The reactions were carried out in 96-well PCR plates using 5 μl of 1:10 diluted cDNA (obtained as described above) in the presence of 12.5 μl of 2$\times$ SoAdvanced universal SYBR green supermix (Bio-Rad), 1 μl of 100 μM forward primer, 1 μl of 100 μM reverse primer, and nuclease-free water to a 25-μl final reaction volume. The cycling parameters were the following: initial denaturation at 95°C for 30 s, followed by 40 amplification cycles of 95°C for 5 s and 60°C for 30 s. Each well was then subjected to a melting curve program (65°C to 95°C at a heating rate of 0.5°C s^{-1}) to confirm specificity of the primers. The expression level of each sample was normalized to the level of the internal control, *rpoD*. Relative expression for each sample was determined using the $2^{-\Delta\Delta CT}$ method. The primers used for RT-qPCR are listed in Table S1. RT-qPCR experiments were carried out on 3 biological replicates per strain, for each condition, with two technical replicates for each sample. Relative expression values are shown as fold difference relative to *fim3* expression in BP536 in the Bvg^- mode (with $MgSO_4$) in Fig. 7.

Statistical analysis. One-way analysis of variance (ANOVA) and unpaired two-tailed *t* test were carried out using Prism 6 software.

Accession number(s). DNA sequences of plasmid vectors described in this study have been deposited in GenBank with accession numbers MH521153 for pSS3967, MH521154 for pSS4162, MH587014 for pQC2123, MH587015 for pQC2319.

SUPPLEMENTAL MATERIAL

Supplemental material for this article may be found at https://doi.org/10.1128/JB.00175-18.

SUPPLEMENTAL FILE 1, PDF file, 4.3 MB.

ACKNOWLEDGMENTS

We thank Kyung Moon for her suggestions and discussion.

This work was funded by the Food and Drug Administration.

REFERENCES

1. CDC. 2017. Pertussis cases by year (1922–2015). Centers for Disease Control and Prevention, Atlanta, GA. https://www.cdc.gov/pertussis/surv-reporting/cases-by-year.html.
2. Mooi FR, Jansen WH, Brunings H, Gielen H, van der Heide HG, Walvoort HC, Guinee PA. 1992. Construction and analysis of Bordetella pertussis mutants defective in the production of fimbriae. Microb Pathog 12:127–135. https://doi.org/10.1016/0882-4010(92)90115-5.
3. Hazenbos WL, van den Berg BM, van't Wout JW, Mooi FR, van Furth R. 1994. Virulence factors determine attachment and ingestion of nonopsonized and opsonized Bordetella pertussis by human monocytes. Infect Immun 62:4818–4824.
4. Cotter PA, Yuk MH, Mattoo S, Akerley BJ, Boschwitz J, Relman DA, Miller JF. 1998. Filamentous hemagglutinin of Bordetella bronchiseptica is required for efficient establishment of tracheal colonization. Infect Immun 66:5921–5929.
5. Mattoo S, Miller JF, Cotter PA. 2000. Role of Bordetella bronchiseptica fimbriae in tracheal colonization and development of a humoral immune response. Infect Immun 68:2024–2033. https://doi.org/10.1128/IAI.68.4.2024-2033.2000.
6. Poolman JT, Hallander HO. 2007. Acellular pertussis vaccines and the role of pertactin and fimbriae. Expert Rev Vaccines 6:47–56. https://doi.org/10.1586/14760584.6.1.47.
7. Stibitz S, Garletts TL. 1992. Derivation of a physical map of the chromosome of Bordetella pertussis Tohama I. J Bacteriol 174:7770–7777. https://doi.org/10.1128/jb.174.23.7770-7777.1992.
8. Parkhill J, Sebaihia M, Preston A, Murphy LD, Thomson N, Harris DE, Holden MT, Churcher CM, Bentley SD, Mungall KL, Cerdeno-Tarraga AM, Temple L, James K, Harris B, Quail MA, Achtman M, Atkin R, Baker S, Basham D, Bason N, Cherevach I, Chillingworth T, Collins M, Cronin A, Davis P, Doggett J, Feltwell T, Goble A, Hamlin N, Hauser H, Holroyd S, Jagels K, Leather S, Moule S, Norberczak H, O'Neil S, Ormond D, Price C, Rabbinowitsch E, Rutter S, Sanders M, Saunders D, Seeger K, Sharp S, Simmonds M, Skelton J, Squares R, Squares S, Stevens K, Unwin L, Whitehead S, Barrell BG, Maskell DJ. 2003. Comparative analysis of the genome sequences of Bordetella pertussis, Bordetella parapertussis and Bordetella bronchiseptica. Nat Genet 35:32–40. https://doi.org/10.1038/ng1227.
9. Locht C, Geoffroy MC, Renauld G. 1992. Common accessory genes for the Bordetella pertussis filamentous hemagglutinin and fimbriae share sequence similarities with the papC and papD gene families. EMBO J 11:3175–3183.
10. Willems RJ, van der Heide HG, Mooi FR. 1992. Characterization of a Bordetella pertussis fimbrial gene cluster which is located directly downstream of the filamentous haemagglutinin gene. Mol Microbiol 6:2661–2671. https://doi.org/10.1111/j.1365-2958.1992.tb01443.x.
11. Willems R, Paul A, van der Heide HG, ter Avest AR, Mooi FR. 1990. Fimbrial phase variation in Bordetella pertussis: a novel mechanism for transcriptional regulation. EMBO J 9:2803–2809.
12. Vaughan TE, Pratt CB, Sealey K, Preston A, Fry NK, Gorringe AR. 2014. Plasticity of fimbrial genotype and serotype within populations of Bordetella pertussis: analysis by paired flow cytometry and genome sequencing. Microbiology 160:2030–2044. https://doi.org/10.1099/mic.0.079251-0.
13. Chen Q, Decker KB, Boucher PE, Hinton D, Stibitz S. 2010. Novel architectural features of Bordetella pertussis fimbrial subunit promoters and their activation by the global virulence regulator BvgA. Mol Microbiol 77:1326–1340. https://doi.org/10.1111/j.1365-2958.2010.07293.x.
14. Cotter PA, Jones AM. 2003. Phosphorelay control of virulence gene expression in Bordetella. Trends Microbiol 11:367–373. https://doi.org/10.1016/S0966-842X(03)00156-2.
15. Boulanger A, Chen Q, Hinton DM, Stibitz S. 2013. In vivo phosphorylation dynamics of the Bordetella pertussis virulence-controlling response regulator BvgA. Mol Microbiol 88:156–172. https://doi.org/10.1111/mmi.12177.
16. Knapp S, Mekalanos JJ. 1988. Two trans-acting regulatory genes (vir and mod) control antigenic modulation in Bordetella pertussis. J Bacteriol 170:5059–5066. https://doi.org/10.1128/jb.170.11.5059-5066.1988.
17. Merkel TJ, Stibitz S. 1995. Identification of a locus required for the regulation of bvg-repressed genes in Bordetella pertussis. J Bacteriol 177:2727–2736. https://doi.org/10.1128/jb.177.10.2727-2736.1995.
18. Merkel TJ, Barros C, Stibitz S. 1998. Characterization of the bvgR locus of Bordetella pertussis. J Bacteriol 180:1682–1690.
19. Herrou J, Bompard C, Wintjens R, Dupre E, Willery E, Villeret V, Locht C, Antoine R, Jacob-Dubuisson F. 2010. Periplasmic domain of the sensor-kinase BvgS reveals a new paradigm for the Venus flytrap mechanism. Proc Natl Acad Sci U S A 107:17351–17355. https://doi.org/10.1073/pnas.1006267107.
20. Dupre E, Wohlkonig A, Herrou J, Locht C, Jacob-Dubuisson F, Antoine R. 2013. Characterization of the PAS domain in the sensor-kinase BvgS: mechanical role in signal transmission. BMC Microbiol 13:172. https://doi.org/10.1186/1471-2180-13-172.
21. Dupre E, Herrou J, Lensink MF, Wintjens R, Vagin A, Lebedev A, Crosson S, Villeret V, Locht C, Antoine R, Jacob-Dubuisson F. 2015. Virulence regulation with Venus flytrap domains: structure and function of the periplasmic moiety of the sensor-kinase BvgS. PLoS Pathog 11:e1004700. https://doi.org/10.1371/journal.ppat.1004700.
22. Dupre E, Lesne E, Guerin J, Lensink MF, Verger A, de Ruyck J, Brysbaert G, Vezin H, Locht C, Antoine R, Jacob-Dubuisson F. 2015. Signal transduction by BvgS sensor-kinase: binding of modulator nicotinate affects conformation and dynamics of entire periplasmic moiety. J Biol Chem 290:23307–23319. https://doi.org/10.1074/jbc.M115.655720.
23. Lesne E, Krammer EM, Dupre E, Locht C, Lensink MF, Antoine R, Jacob-Dubuisson F. 2016. Balance between coiled-coil stability and dynamics regulates activity of BvgS sensor kinase in Bordetella. mBio 7:e02089. https://doi.org/10.1128/mBio.02089-15.
24. Lesne E, Dupre E, Locht C, Antoine R, Jacob-Dubuisson F. 2017. Conformational changes of an interdomain linker mediate mechanical signal transmission in sensor kinase BvgS. J Bacteriol 199:e00114-17. https://doi.org/10.1128/JB.00114-17.
25. Lesne E, Dupre E, Lensink MF, Locht C, Antoine R, Jacob-Dubuisson F. 2018. Coiled-coil antagonism regulates activity of venus flytrap-domain-containing sensor kinases of the BvgS family. mBio 9:e02052-17. https://doi.org/10.1128/mBio.02052-17.
26. Lacey BW. 1960. Antigenic modulation of Bordetella pertussis. J Hyg (Lond) 58:57–93. https://doi.org/10.1017/S0022172400038134.
27. Croinin TO, Grippe VK, Merkel TJ. 2005. Activation of the vrg6 promoter of Bordetella pertussis by RisA. J Bacteriol 187:1648–1658. https://doi.org/10.1128/JB.187.5.1648-1658.2005.
28. Stenson TH, Allen AG, Al-Meer JA, Maskell D, Peppler MS. 2005. Bordetella pertussis risA, but not risS, is required for maximal expression of

Bvg-repressed genes. Infect Immun 73:5995–6004. https://doi.org/10.1128/IAI.73.9.5995-6004.2005.
29. Chen Q, Ng V, Warfel JM, Merkel TJ, Stibitz S. 2017. Activation of Bvg-repressed genes in Bordetella pertussis by RisA requires cross-talk from a noncooperonic histidine kinase RisK. J Bacteriol 199:e00475-17. https://doi.org/10.1128/JB.00475-17.
30. Hot D, Antoine R, Renauld-Mongenie G, Caro V, Hennuy B, Levillain E, Huot L, Wittmann G, Poncet D, Jacob-Dubuisson F, Guyard C, Rimlinger F, Aujame L, Godfroid E, Guiso N, Quentin-Millet MJ, Lemoine Y, Locht C. 2003. Differential modulation of Bordetella pertussis virulence genes as evidenced by DNA microarray analysis. Mol Genet Genomics 269:475–486. https://doi.org/10.1007/s00438-003-0851-1.
31. Cummings CA, Bootsma HJ, Relman DA, Miller JF. 2006. Species- and strain-specific control of a complex, flexible regulon by Bordetella BvgAS. J Bacteriol 188:1775–1785. https://doi.org/10.1128/JB.188.5.1775-1785.2006.
32. Moon K, Bonocora RP, Kim DD, Chen Q, Wade JT, Stibitz S, Hinton DM. 2017. The BvgAS regulon of Bordetella pertussis. mBio 8:e01526-17. https://doi.org/10.1128/mBio.01526-17.
33. Diavatopoulos DA, Cummings CA, Schouls LM, Brinig MM, Relman DA, Mooi FR. 2005. Bordetella pertussis, the causative agent of whooping cough, evolved from a distinct, human-associated lineage of B. bronchiseptica. PLoS Pathog 1:e45. https://doi.org/10.1371/journal.ppat.0010045.
34. Chen Q, Boulanger A, Hinton DM, Stibitz S. 2014. Strong inhibition of fimbrial 3 subunit gene transcription by a novel downstream repressive element in Bordetella pertussis. Mol Microbiol 93:748–758. https://doi.org/10.1111/mmi.12690.
35. Mooi FR, ter Avest A, van der Heide HG. 1990. Structure of the Bordetella pertussis gene coding for the serotype 3 fimbrial subunit. FEMS Microbiol Lett 54:327–331. https://doi.org/10.1111/j.1574-6968.1990.tb04021.x.
36. Cummings CA, Brinig MM, Lepp PW, van de Pas S, Relman DA. 2004. Bordetella species are distinguished by patterns of substantial gene loss and host adaptation. J Bacteriol 186:1484–1492. https://doi.org/10.1128/JB.186.5.1484-1492.2004.
37. Stibitz S, Yang MS. 1991. Subcellular localization and immunological detection of proteins encoded by the vir locus of Bordetella pertussis. J Bacteriol 173:4288–4296. https://doi.org/10.1128/jb.173.14.4288-4296.1991.
38. Miller JH. 1972. Experiments in molecular genetics. Cold Spring Harbor Laboratory Press, Cold Spring Harbor, NY.
39. Hinton DM. 1989. Transcript analyses of the uvsX-40-41 region of bacteriophage T4. Changes in the RNA as infection proceeds. J Biol Chem 264:14432–14439.
40. Guild N, Gayle M, Sweeney R, Hollingsworth T, Modeer T, Gold L. 1988. Transcriptional activation of bacteriophage T4 middle promoters by the motA protein. J Mol Biol 199:241–258. https://doi.org/10.1016/0022-2836(88)90311-7.
41. Hinton DM. 1991. Transcription from a bacteriophage T4 middle promoter using T4 motA protein and phage-modified RNA polymerase. J Biol Chem 266:18034–18044.
42. Bonocora RP, Caignan G, Woodrell C, Werner MH, Hinton DM. 2008. A basic/hydrophobic cleft of the T4 activator MotA interacts with the C-terminus of E. coli sigma70 to activate middle gene transcription. Mol Microbiol 69:331–343. https://doi.org/10.1111/j.1365-2958.2008.06276.x.
43. James TD, Cashel M, Hinton DM. 2010. A mutation within the beta subunit of Escherichia coli RNA polymerase impairs transcription from bacteriophage T4 middle promoters. J Bacteriol 192:5580–5587. https://doi.org/10.1128/JB.00338-10.
44. Sanger F, Nicklen S, Coulson AR. 1977. DNA sequencing with chain-terminating inhibitors. Proc Natl Acad Sci U S A 74:5463–5467. https://doi.org/10.1073/pnas.74.12.5463.
45. Simon R, Priefer U, Pühler A. 1983. A broad host range mobilization system for in vivo genetic engineering: transposon mutagenesis in gram negative bacteria. Nat Biotechnol 1:784–791. https://doi.org/10.1038/nbt1183-784.
46. Lopez CM, Rholl DA, Trunck LA, Schweizer HP. 2009. Versatile dual-technology system for markerless allele replacement in Burkholderia pseudomallei. Appl Environ Microbiol 75:6496–6503. https://doi.org/10.1128/AEM.01669-09.
47. Kasuga T, Nakase Y, Ukishima K, Takatsu K. 1954. Studies on Haemophilus pertussis. V. Relation between the phase of bacilli and the progress of the whooping-cough. Kitasato Arch Exp Med 27:57–62.